FINAL WORK PLAN FOR
CO$_2$ SPARGING
PROOF OF CONCEPT TEST

LCP CHEMICAL SITE, BRUNSWICK, GA

Prepared for Honeywell

Prepared by:

Mutch Associates, LLC

360 Darlington Avenue

Ramsey, NJ 07446

In collaboration with:

Parsons

3577 Parkway Lane, Suite 100

Norcross, GA 30309

September 11, 2012

Table of Contents

List of Tables

List of Figures

List of Acronyms

Alk	Alkalinity
bgs	Below ground surface
CBP	Caustic brine pool
CO_2	Carbon dioxide
$CO_2(aq)$	Aqueous carbon dioxide
$CO_2(g)$	Gaseous carbon dioxide
CO_3^{2-}	Carbonate ion
Cr(III)	Trivalent chromium
Cr(VI)	Hexavalent chromium
DIC	Dissolved inorganic carbon
DO	Dissolved oxygen
DOC	Dissolved organic carbon
DOM	Dissolved organic matter
E_h	Redox potential relative to the Standard Hydrogen Electrode
ESTCP	Environmental Security Technology Certification Program
GEPD	Georgia Environmental Protection Division
H	Henry's Law Constant
$H_2CO_3(aq)$	Carbonic acid
H_2CO_3*	Sum of carbonic acid and aqueous carbon dioxide
HCO_3^-	Bicarbonate ion
H_2SO_4	Sulfuric acid
Hg	Mercury
IDW	Investigation derived waste
k	Kinetic rate constant
K	Equilibrium constant
K_h	Hydraulic conductivity
K_{sp}	Solubility product constant
LCP	Linden Chemicals and Plastics
NTU	Nepholometric Turbidity Unit
ORP	Oxidation Reduction Potential
psi	Pounds per square inch
psig	Pounds per square inch – gauge
PVC	Poly vinyl chloride
Q	Reaction quotient
R_{tot}	Total or overall rate of dissolution
RAO	Remedial Action Operation
RI	Remedial Investigation
ROI	Radius of influence
scfm	Standard cubic feet per minute
SC	Specific conductivity
SI	Saturation index
$SF_6(aq)$	Aqueous sulfur hexafluoride
$SF_6(g)$	Gaseous sulfur hexafluoride
TAL	Target Analyte List
TDS	Total dissolved solids
TSS	Total suspended solids

1. INTRODUCTION

In 2010, CH2M Hill prepared a work plan on behalf of Honeywell International (Honeywell) for a pilot test of carbon dioxide (CO_2) sparging to neutralize pH and reduce density of the Caustic Brine Pool (CBP) (CH2M Hill, 2010). This test involved multiple CO_2 injection points with multiple vertical intervals at each location and hydraulic fracturing. In September of 2010, USEPA Region 4 raised a number of concerns and questions regarding the proposed technology. Mutch Associates, LLC, (Mutch Associates) and Parsons were retained by Honeywell to evaluate whether those concerns can be addressed and whether this technology has merit for addressing pH and density of the CBP at the Brunswick, Georgia Linden Chemicals and Plastics (LCP) Chemical site. In so doing, we conducted a laboratory study of CO_2 sparging of representative samples of the CBP, researched other applications of the technology, conducted a geochemical assessment of potential dolomite dissolution, and evaluated other delivery methods of CO_2 besides the earlier-proposed hydraulic fracturing.

This work plan is structured in the following manner. Section 2, which follows, reiterates and addresses the questions and concerns expressed by USEPA relative to the 2010 work plan. This section also describes our laboratory study of CO_2 sparging and sets forth the technical approach for a smaller-scale proof of concept test that we believe addresses the agencies' concerns raised in connection with the proposed 2010 pilot scale study. Section 3 presents a detailed description of the work elements comprising the proof of concept test, including construction of the proposed monitoring well network, pre-injection aquifer testing and monitoring, carbon dioxide injection, monitoring during carbon dioxide injection, post injection monitoring, and post injection aquifer testing. Section 4 describes how the data would be evaluated and reported. A proposed schedule is presented in Section 5, assuming approval for implementation of the proof of concept test is received from the USEPA and Georgia Environmental Protection Division (GEPD). Lastly, Section 6 provides a list of references used in preparation of this work plan.

2 TECHNICAL APPROACH

In 2010, a work plan, entitled, "Draft Pilot Test Work Plan, Caustic Brine Pool In-situ Treatment, LCP Chemical site, Brunswick GA" (CH2M Hill, 2010) was submitted to USEPA and GEPD for their review. This work plan proposed a large-scale pilot test of CO_2 sparging aimed at reducing pH and density within the CBP. The proposed pilot test involved hydraulic fracturing, multiple sparge locations, multiple sparge/fracturing depths at each location, and sparging of up to 1500 scfm at each sparge point in the subsurface. USEPA and GEPD raised a number of concerns relative to this proposed pilot test. In this section, we will address those concerns in some detail. We address those concerns in several ways:

1. First, we offer a different technical approach to conduct a pilot test, one that is best termed a "proof of concept" test. The proposed proof of concept test would involve a single sparge point, would <u>not</u> involve hydraulic fracturing, would sparge CO_2 at a small fraction of the rates proposed in the 2010 work plan, would intermittently pulse in CO_2 to gradually approach pH target levels, and would continuously monitor pH during the test. A comparison of key features of the 2010 Pilot Test and this proposed proof of concept test is presented in Table 2-1.

Table 2-1

Comparison of 2010 Pilot Test and 2012 Proof of Concept Test

Feature	Proposed 2010 Pilot Test	Proposed 2012 Proof of Concept Test
Injection locations	4	1
Injection intervals per location	5 to 8	1
Planned injection rate at each vertical interval	750-1500 scfm	20 scfm
In situ fracturing	Yes	No
Monitoring pH changes during the CO_2 sparging	None (just before and after)	Continuous pH dataloggers
Monitoring of water table mounding	None	Continuous Solinst water level dataloggers
Rebound monitoring	pH only	pH, DIC, alkalinity, TDS, dissolved silica, TAL metals

2. Second, we have conducted a laboratory study of CO_2 sparging into CBP waters to better assess any issues potentially relating to solids precipitation during in situ CO_2 sparging.

2

3. Third, we have conducted literature research and technical analyses of other concerns raised by USEPA and GEPD in connection with the 2010 work plan.

We begin by addressing the specific concerns raised by USEPA and GEPD in connection with the 2010 work plan.

In its September 7, 2010, comments on the "Draft Pilot Test Work Plan, Caustic Brine Pool In-situ Treatment, LCP Chemical site, Brunswick GA" USEPA raised a number of concerns that are listed or paraphrased below:

1. In-situ CO_2 injection, coupled with fracturing, appears to be a very innovative and essentially untested technology for its apparent intended use at the site as an in-situ sparging method. (*This was addressed by undertaking a laboratory CO_2 sparging study, and by identifying a sparging case study as discussed in Sections 2.1 and 2.2*).

2. In-situ precipitation of silica appears to be a potentially significant problem. The rapid plugging of injection sites is a definite possibility as noted by GEPD. Permeability reductions in the areas surrounding injection sites could further reduce the likelihood of uniform distribution of CO_2. (*This was addressed using the results from the sparging study which is discussed in Section 2.4*).

3. Insufficient information was available to assess the impact of silica precipitation on the metals contaminants in the CBP. The permanence of any metals and mobilization or precipitation due to silica gel formation is uncertain. (*Data from the recent literature on mercury geochemistry was used to address this in Section 2.7*).

4. Injection of CO_2 gas into the saturated subsurface of the CBP raises many of the same issues as air sparging. These issues include migration of gas in channels that bypass much of the matrix, uneven distribution of gas, limited radius of influence as migration would be primarily vertically upward, and limited mixing of CO_2 into a significant portion of the subsurface. In addition, the impact of the fracturing method on CBP migration and stability are unclear. (*The proposed proof of concept test will evaluate the extent and uniformity of CO_2 distribution. This is discussed in Sections 3.7 and 3.8*).

5. The CO_2 sparging would increase dissolution of the dolomitic-cemented sandstone. (*This was assessed through thermodynamic and kinetic modeling calculations in Section 2.3*).

6. In-situ injection of CO_2 gas might tend to provide a driving force for increased advection of subsurface fluids, which could increase brine and contaminant migration vertically as well as horizontally. (*This was addressed through groundwater flow calculations in Section 2.5*).

7. A thorough geochemical evaluation of the interactions of the CO_2 injection and metals, and how the CO_2 injection affects RAOs for metals (if any), appears important, given the numerous geochemical changes to be expected. (*The influence of CO_2 on the geochemistry of Hg, As, and Cr is addressed in Section 2.7.1*).

8. If in-situ treatment by CO_2 sparging were used, it is possible that the area around each CO_2 injection well might be geochemically very different. The loading of CO_2 into each of these areas, and the effects of the CBP, might be different. This would complicate the applicability of the pilot-study information to full scale, increase the complexity of the subsurface treatment, and make it more problematic to achieve immediate goals. (*The proposed proof of*

3

concept test will evaluate the heterogeneities of the post-sparging geochemical conditions in the CBP. This is discussed in Sections 3.7 and 3.8.)

9. Uncontrolled off-gassing of CO_2 is a concern in terms of worker safety. (*This will be addressed in the field by monitoring for CO_2 and other vapors as described in Section 2.6*).

We believe that each of the above-listed concerns of USEPA and GEPD are addressed either by the laboratory study conducted as part of this work plan development and described herein, by more extensive research of particular issues, by the very different design of the proposed proof of concept test, itself, or through implementation of the proof of concept test to answer questions that can only be answered through a carefully designed, safe, and well-instrumented field test. As we go through the technical approach for the CO_2 proof of concept test, the manner in which we address each of the above concerns will be described.

Specific objectives of the proof of concept test include:

- Determine the radius of influence (ROI) of a representative CO_2 sparging well as defined by pH reduction to target levels
- Determine the kinetics of the pH neutralization reaction
- Determine the efficiency of the CO_2 sparging as defined by the amount of pH reduction achieved per mass of CO_2 injected
- Assess whether any significant reductions in aquifer hydraulic conductivity occur within the ROI as a result of the CO_2 sparging
- Assess whether there is any significant reduction in the specific capacity of the sparge well, which will also serve as the aquifer testing groundwater extraction well before and after the CO_2 sparging test
- Determine the impact of the CO_2 sparging on the geochemistry of the aquifer within the ROI and in particular on the concentrations of mercury and other metals
- Determine the vertical magnitude, radial extent, rate of propagation, and life-cycle of any groundwater mounding caused by the CO_2 sparging and the extent of groundwater level collapse following cessation of sparging
- Determine practical CO_2 injection rates and ways in which sparging efficiency can be enhanced
- Monitor over time any rebound in pH, metals, or other geochemical parameters

2.1 Lab Study of CO_2 Sparging

A CO_2 sparging laboratory study was conducted in April, 2012 by Mutch Associates, LLC. The purpose of the test was to i) determine the pH response of CBP water upon sparging with $CO_2(g)$, and ii) assess the extent of solids production upon pH adjustment with $CO_2(g)$. Approximately 2.0 L of groundwater from EW-4, EW-6 and EW-10 were collected by CH2M Hill for testing. The locations of these extraction wells are depicted on Figure 2-1. These wells were selected to cover a range of geochemical conditions found in the CBP based upon results of sulfuric acid titrations (2009) and recent GW quality data (2011): EW-10 (low acid demand, pH 11.23, low dissolved silicon), EW-4 (medium acid demand, pH 11.73, med dissolved silicon), and EW-6 (high acid demand, pH 11.49, high dissolved silicon).

Samples were analyzed pre-sparging for pH, dissolved metals, dissolved silicon, alkalinity and TDS. These results are summarized in Table 2-2.

Table 2-2. Pre-Sparging Chemical Characteristics of CBP Samples used in Laboratory Sparge Test

	EW-4	EW-6	EW-10	
pH	10.90	12.25	11.37	
Alkalinity	2,160	10,300	2,810	mg/L as $CaCO_3$
TDS	7,220	49,400	11,000	mg/L
Si	359	379	168	mg/L
Hg	204	617	138	µg/L
Cr	261	299	305	µg/L
As	53	358	69	µg/L
Na	1,910	14,400	2,690	mg/L
Fe	4.37	7.37	2.40	mg/L

Note: pH values in table were measured in the laboratory just prior to sparge test.

The experimental set-up is shown in Figure 2-2. Compressed $CO_2(g)$ was bubbled through a fine bubble diffuser into 500 mL of CBP water at a flow rate of 0.50 L/min. A pH electrode recorded the pH as a function of time. At the end of the test, the water was filtered through a 0.45 µm filter and sent to Accutest Laboratories (Dayton, NJ) for analysis of dissolved silicon, TDS, and alkalinity.

For all three CBP water samples, the pH dropped quickly (within a few minutes) and a pH of between 6.5 and 7.0 was achieved. Titration curves showing pH versus sparging time are shown in Figure 2-3. Once the pH reached approximately 7.0, further sparging resulted in relatively small decreases in pH. Prolonged sparging with CO_2 achieved a pH of 6.5 in EW-4 and EW-10. Prolonged sparging of EW-6 did not lower pH below 6.7. The pH stayed relatively constant at these values hours after sparging ceased.

Sparging of all three waters was accompanied by foaming (Figure 2-4). Visually, there was no evidence of solid formation in EW-4 and EW-10 up to 6 hours after sparging (Figure 2-5). Total suspended solids (TSS) measurements on EW-4 and EW-10 resulted in 31 mg/L and 26 mg/L respectively. The sparged water was placed in separatory funnels to monitor solids formation over time. There was no visual evidence of solids formation up to 6 weeks after the test.

Sparging of EW-6 initially did not produce any solids. However, continued sparging to a pH less than approximately 7 resulted in formation of a brown gelatinous solid material (Figure 2-6). The TSS of the water after sparging was 13.9 g/L. The % volatile content of the suspended solid was 10% based upon ignition at 550°C. Analytical data revealed that sparging lowered the total silicon from 379 to 38 mg/L. This indicates that the material is silicon based and is most likely "gelatinous silica", a hydrated amorphous silica solid that is known to form when highly concentrated solutions of dissolved silicon are acidified to pH less than 7.

2.2 Case Studies of CO_2 Sparging

The most relevant case study is a CO_2 sparging pilot test that was performed in 2009 by McCue Environmental Contracting, Inc. at an undisclosed site on the western coast of Canada. The goal of the

test was to determine the effectiveness of CO_2 sparging on lowering the pH of a caustic groundwater plume. The highest pH value reported at the site was 13.33, while most of the pH values within the caustic plume were approximately between 12 and 13. These pH values are similar to those observed in the CBP in the Satilla Sand formation. The aquifer was highly permeable with a hydraulic conductivity of approximately 10^{-1} cm/s.

A total of 11 tests were conducted in three sparge wells over an approximate 15 day period. CO_2 was sparged at shallow (7 to 36 ft bgs), intermediate (36 to 69 ft bgs), and deep (> 69 ft bgs) depths at the same location. These depths corresponded to freshwater, transition and saline zones. At the shallow depth, 5 to 9 psig was applied at flow rates up to 8 scfm. At the intermediate depth, 15 to 19 psig was applied at flow rates up to 15 scfm. At the deep depth, 28 to 41 psig was applied, at flow rates from 36 to 85 scfm. The maximum pressure employed to achieve sparging at the deepest depth was 41 psig (125% of the static pressure head).

The results of the pilot test were extremely positive. A pH reduction was observed in monitoring wells screened in both shallow and intermediate zones. The pH decreased from 11.14 to 6.43 in the shallow monitoring well, while the pH decreased from 13.21 to 6.17 in the intermediate monitoring well. The monitoring well was located 8 m (26 ft) away from the sparge well. The time required to observe the lowered pH varied from 15 minutes to 60 minutes from start of the test. There was no pH decrease observed in the deep monitoring well. The pH stayed low in the majority of monitoring wells up to 1 year after the test. There was no evidence of solids formation in the sparging wells, and there was no significant difference in hydraulic conductivity pre- and post-testing.

A study performed at the ZERT field site in Bozeman, Montana by Kharaka et al. (2010) also has relevance to the Proof of Concept Test. In this study, approximately 300 kg/d of food grade CO_2 was injected into a horizontal perforated pipe located 2.0 to 2.3 m (6.6 to 7.5 ft) below the ground. The purpose of the test was to evaluate atmospheric and near surface monitoring and detection techniques for use in subsurface storage of CO_2. Groundwater samples were collected from 10 monitoring wells screened separately at shallow (1.5 m, 4.9 ft) and deep (3.0 m, 9.8 ft) intervals. CO_2 was injected for approximately 1 month. Within a day of sparging, the pH decreased from 7.0 to approximately 6.0 in three nearby monitoring wells. The lowest pH (5.6) was observed in a monitoring well 1 m (3.2 ft) from the injection pipe after three weeks of sparging.

Alkalinity and major ions were also monitored during CO_2 injection. Alkalinity increased from approximately 400 mg/L to 1,200 mg/L as HCO_3^- after injection. This increase in alkalinity was accompanied by an increase in Ca^{2+} and a modest increase in Mg^{2+}. This data was interpreted as evidence for dissolution of carbonate solids. To account for the observed increase in Mg^{2+}, Kharaka et al. (2010) suggested Mg-rich calcite and/or dolomite dissolution. These results indicate the need for careful control of the pH to avoid it falling below 6.0 and potential dissolution of carbonate-bearing solids.

2.3 Analysis of Potential for Aquitard Dolomitic Cement Dissolution

The potential for dissolution of the dolomitic sandstone aquitard was assessed through thermodynamic and kinetic rate calculations is described in this section. Section 2.3.1 contains a review of background material related to carbon dioxide chemistry and the results of a literature review on dolomite dissolution. Section 2.3.2 describes calculations performed to assess the threat of dolomite

6

dissolution after pH neutralization. Multiple lines of evidence are presented indicating that conditions after sparging will not promote dolomite dissolution.

2.3.1 Background/Literature Review

Sparging with $CO_2(g)$ imparts dissolved inorganic carbon species to the water and increases the H^+ concentration (i.e. lowers the pH):

$$CO_2(g) \rightleftharpoons CO_2(aq) \tag{2.1}$$

$$CO_2(aq) + H_2O(l) \rightleftharpoons H_2CO_3(aq) \tag{2.2}$$

$$H_2CO_3(aq) \rightleftharpoons H^+ + HCO_3^- \tag{2.3}$$

In the above reactions, $CO_2(aq)$ is aqueous carbon dioxide, $H_2CO_3(aq)$ is carbonic acid, and HCO_3^- is the bicarbonate ion. Under all pH conditions, $CO_2(aq)$ is dominant over $H_2CO_3(aq)$ as indicated by the small value for the equilibrium constant (1.6×10^{-3}) for reaction 2.2. As a result, it is has become accepted for $CO_2(aq)$ and $H_2CO_3(aq)$ to be combined into one species known as $H_2CO_3^*$. Thus, the concentration of $H_2CO_3^*$ is obtained by summing the concentration of $CO_2(aq)$ and $H_2CO_3(aq)$. For the purposes of performing equilibrium speciation calculations, the above reactions are modified to incorporate $H_2CO_3^*$:

$$CO_2(g) + H_2O(l) \rightleftharpoons H_2CO_3* \qquad K_{CO_2} = 3.39 \times 10^{-2} \ (25°C) \tag{2.4}$$

$$H_2CO_3* \rightleftharpoons H^+ + HCO_3^- \qquad K_{a1} = 4.45 \times 10^{-7} (25°C) \tag{2.5}$$

Note that $CO_2(aq)$ and $H_2CO_3(aq)$ do not appear in Equations 2.4 and 2.5. A second acid base reaction results as bicarbonate ion deprotonates to form carbonate ion:

$$HCO_3^- \rightleftharpoons H^+ + CO_3^{2-} \qquad K_{a2} = 4.69 \times 10^{-11} (25°C) \tag{2.6}$$

The distribution of inorganic carbon species amongst $H_2CO_3^*$, HCO_3^- and CO_3^{2-} is a function of the pH of the water. $H_2CO_3^*$ is dominant below pH 6.3, HCO_3^- is dominant between pH 6.3 and 10.3, and CO_3^{2-} is dominant above pH 10.3. The pH regime of maximum buffering ability is at pH values close to the values of pK_{a1} and pK_{a2} (i.e. pH = 6.3 and 10.3)

Dissolution of dolomite has been studied extensively and the conditions which promote dolomite dissolution are well understood. The solubility of dolomite is described by the following (Martell et al., 2004):

$$CaMg(CO_3)_2(s, dolomite) \rightleftharpoons Ca^{2+} + Mg^{2+} + 2CO_3^{2-} \qquad K_{sp} = 10^{-17.0} \tag{2.7}$$
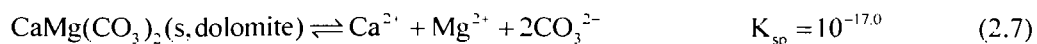
It is generally believed that, like calcite, dolomite dissolution can be described by three parallel reactions occurring at the solid/water interface (Chou et al., 1989; Plummer et al., 1978):

$$CaMg(CO_3)_2(s) + 2H^+ \xrightarrow{k_1} Ca^{2+} + Mg^{2+} + 2HCO_3^- \tag{2.8}$$

$$CaMg(CO_3)_2(s) + 2H_2CO_3* \xrightarrow{k_2} Ca^{2+} + Mg^{2+} + 4HCO_3^- \tag{2.9}$$

$$CaMg(CO_3)_2(s) \underset{k_4}{\overset{k_3}{\rightleftharpoons}} Ca^{2+} + Mg^{2+} + 2CO_3^{2-} \tag{2.10}$$
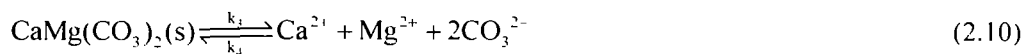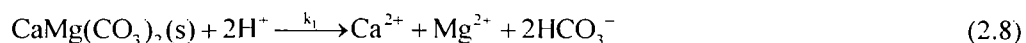
According to this mechanism, the surface area normalized dissolution rate of dolomite has been described by the following (Busenberg and Plummer, 1982; Morse and Arvidson, 2002):

$$R_{tot} = k_1 \{H^+\}^n + k_2 \{H_2CO_3^*\}^{0.5} + k_3 \{H_2O\}^{0.5} - k_4 \{CO_3^{2-}\}$$
$$R_{tot} = R_1 + R_2 + R_3 - R_4$$

(2.11)

where R_{tot} represents the total or overall rate of dissolution (in mol/cm^2-s). The exponent n has been shown to vary from 0.5 (Busenberg and Plummer, 1982) to 0.75 (Chou et al., 1989). Within this mechanistic scheme, the first term in Equation 2.11 corresponds to dolomite surface protonation, the second to its carbonatation, the third to surface hydration, and the fourth term accounts for the precipitation reaction. Rate constants at 25 °C for k_1 through k_4 are 1.7×10^{-8}, 4.3×10^{-10}, 2.5×10^{-13} (with units of $L^{0.5}mol^{0.5}cm^{-2}s^{-1}$) and 2.8×10^{-8} L/cm^2-s respectively.

Pokrovsky et al. (1999) developed a surface complexation model that was able to shed light on the first term in Equation 2.11. They proposed that the surface of dolomite consisted of surface sites of the form $>CO_3^-$ which can undergo exchange reactions with H^+, Ca^{2+} and Mg^{2+} from solution. For example:

$$>CO_3^- + H^+ \rightleftharpoons >CO_3H^0 \qquad K_{int} = 10^{-4.8}$$

(2.12)
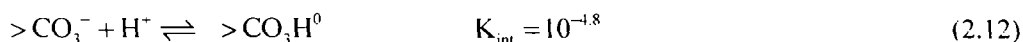
The reaction above indicates that $>CO_3H^0$ increases with decreasing pH and that $>CO_3H^0$ is preferred over $>CO_3^-$ at pH < 4.8. Pokrovsky et al. (1999) attributed the enhancement of dolomite dissolution rate by H^+ at pH < 6 to the protonation of the dolomite surface. Within the surface coordination approach, the dolomite proton-promoted dissolution rate was expressed as:

$$R_1 = k_{CO_3} \{>CO_3H^0\}^2$$

(2.13)

This rate equation adequately describes dolomite dissolution over a wide range of solution conditions at pH < 6.

At neutral to alkaline conditions, the hydration of surface metal sites controls the rate of this mechanism as described by the third term in Equation 2.11 (Pokrovsky et al., 1999). The first step of dolomite dissolution is the preferential release of Ca^{2+} from dolomite with formation of $>MgCO_3^-$, a magnesium surface site (Pokrovsky and Schott, 2001):

$$>Ca(Mg)CO_3^+ \rightleftharpoons >MgCO_3^- + Ca^{2+} \qquad K_{Ca}^*$$

(2.14)
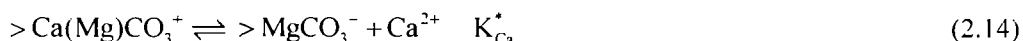
The second slow (i.e. rate controlling) step is the hydration of exposed Mg surface sites which is the same as similar in form to the rate law that governs magnesite ($MgCO_3(s)$) dissolution:

$$>MgCO_3^- + H_2O \rightleftharpoons >MgOH_2^+ + CO_3^{2-} \qquad K_{CO_3}^*$$

(2.15)

Dolomite dissolution rates (under far from equilibrium conditions) versus $\{>MgOH_2^+\}$ on a logarithmic scale were linear with a slope equal to 1.9, this suggesting that the rate can be described by:

$$R_3 = k_{Mg}^+ \{>MgOH_2^+\}^{1.9}$$

(2.16)

where k_{Mg}^+ is the forward rate constant (1.12×10^5 mol^{-1} cm^2 s^{-1}) and $\{>MgOH_2^+\}$ is the activity of the hydrated magnesium surface site. The activity of $>MgOH_2^+$ can be calculated using the dolomite surface

8

speciation model of Pokrovsky et al. (1999). By assuming the total number of dolomite surface sites is a constant value (7×10^{-6} mol/m^2), an alternate expression was derived for the rate (Pokrovsky and Schott, 2001):

$$R_3 = k_{Mg}^* \left(\frac{K_{CO_3}^* K_{Ca}^*}{K_{CO_3}^* K_{Ca}^* + K_{Ca}^* \{CO_3^{2-}\} + \{CO_3^{2-}\} \{Ca^{2+}\}} \right)^{1.9} \qquad (2.17)$$

$K^*_{CO_3}$ and K^*_{Ca} are equilibrium constants for the formation of surface complexes according to Equations 2.14 and 2.15. The constant k^*_{Mg} is a surface area normalized rate constant equal to 6.3×10^{-13} mol cm^{-2} s^{-1}. The above equation shows that the dissolution rate is inversely proportional to the activities of CO_3^{2-} and Ca^{2+}. In other words, Ca^{2+} and CO_3^{2-} impart a protective effect on dolomite dissolution. The above equation is essentially an improvement upon term R_3 of Busenberg and Plummer (1982).

Using Transition State Theory (TST), (Pokrovsky and Schott, 2001), have provided a rate expression which accounts for dissolution and precipitation of dolomite at neutral pH:

$$R = k_{Mg}^* \left(\frac{K_{CO_3}^* K_{Ca}^*}{K_{CO_3}^* K_{Ca}^* + K_{Ca}^* \{CO_3^{2-}\} + \{CO_3^{2-}\} \{Ca^{2+}\}} \right)^{1.9} \left(1 - \left(\frac{Q}{K_{sp}} \right)^{1.9} \right) \qquad (2.18)$$

where, Q represents the reaction quotient. The logarithm of the ratio of Q to K_{sp} is often referred to as the saturation index, a measure of whether a solution is undersaturated or undersaturated with respect to a particular solid phase. When $Q \ll K_{sp}$, the system is under "far from equilibrium conditions", and the second term reduces to 1. When Q is only slightly less than 1, the second term attenuates the dissolution rate calculated by the first term. When $Q > K_{sp}$, the second term is negative, and Equation 2.18 provides a negative dissolution rate which indicates conditions which favor precipitation of dolomite.

2.3.2 Potential for Dolomitic Sandstone Dissolution Upon Sparging with CO_2

By imparting a large amount of inorganic carbon to the water, there will be a large amount of pH buffering achieved once the pH drops below pH 7.0. This is clearly evident in the $CO_2(g)$ titrations shown in Figure 2-3 for EW-4, EW-6 and EW-10. Prolonged sparging with $CO_2(g)$ did not lower the pH below 6.5.

Generally, it has been observed that dolomite dissolution is about 100 times slower than dissolution of calcite or magnesite and that relatively small concentrations of carbonate can almost completely suppress dolomite dissolution (Busenberg and Plummer, 1986). Ca^{2+} is also known to have an inhibitory effect on dolomite dissolution (Pokrovsky and Schott, 2001). The following sections provide a formal quantitative assessment of the potential for dolomite dissolution upon pH adjustment of the CBP.

2.3.2.1 Thermodynamic Assessment

The solubility of dolomite is governed by the reaction shown in Equation 2.7. The saturation index (SI) was used to determine whether conditions favor or disfavor dissolution of dolomite. The SI for dolomite was calculated according to the following:

$$SI = \log \left(\frac{Q}{K_{sp}} \right) = \log \left(\frac{\{Ca^{2+}\} \{Mg^{2+}\} \{CO_3^{2-}\}^2}{K_{sp}} \right) \qquad (2.19)$$

9

When the SI is less than 0, dissolution of a solid phase is predicted so as to maintain thermodynamic equilibrium. A plot of the SI for dolomite versus pH is shown for site groundwater from 2010 (Figure 2-7). The SI is greater than or equal to 0 whenever the pH is greater than 7.5, indicating that dolomite dissolution is not thermodynamically favorable under these conditions. Between pH 6.5 and 7.5, the SI varies between −3.0 and 1.8.

A negative SI for dolomite is not expected at pH 7.5 and above, and therefore the groundwater is expected to be supersaturated with respect to dolomite. The laboratory study has shown that it required prolonged sparging to decrease the pH below 7.0 and that it will not decrease the pH below 6.5. Even if the SI were to drop below 0, dissolution of dolomite is severely limited at saturation indices greater than −3.0 (Pokrovsky and Schott, 2001). As the pH decreases, the activity of CO_3^{2-} naturally decreases to maintain the equilibria described by Equations 2.5 and 2.6. However, since the pH decrease will be achieved by an increase in DIC, the effect on the CO_3^{2-} activity will not be as severe as if a mineral acid such as hydrochloric or sulfuric acid was used for pH adjustment. This will further help prevent the SI for dolomite from becoming negative.

2.3.2.2 Kinetic Assessment

The kinetic model of Busenberg and Plummer (1982) was employed to assess the potential for dolomite dissolution. The final pH, TDS, and alkalinity resulting from the CO_2 sparging laboratory test was used to calculate the activities of H^+, $H_2CO_3^*$, and HCO_3^-. These quantities were then used to calculate the four terms in Equation 2.11. These results are summarized in Table 2-3.

Table 2-3. Calculations of kinetic rates of dolomite dissolution using the model of Busenberg and Plummer (1982)

	EW-4	EW-6	EW-10	
Final pH	6.5	6.7	6.5	
Alkalinity	2,270	10,000	2,770	mg/L as $CaCO_3$
H^+ activity	1.39×10^{-7}	2.19×10^{-7}	2.19×10^{-7}	mol/L
$H_2CO_3^*$ activity	4.29×10^{-2}	1.54×10^{-2}	1.88×10^{-2}	mol/L
HCO_3^- activity	1.38×10^{-1}	3.14×10^{-2}	3.83×10^{-2}	mol/L
R_1	6.32×10^{-12}	7.95×10^{-12}	7.95×10^{-12}	mol/cm^2-s
R_2	8.90×10^{-11}	5.34×10^{-11}	5.90×10^{-11}	mol/cm^2-s
R_3	2.50×10^{-13}	2.50×10^{-13}	2.50×10^{-13}	mol/cm^2-s
R_4	-3.87×10^{-9}	-8.78×10^{-10}	-1.07×10^{-9}	mol/cm^2-s
R_{tot}	-3.77×10^{-9}	-8.17×10^{-10}	-1.00×10^{-9}	mol/cm^2-s

For all three waters, the total or net dissolution rate was negative, indicating that conditions are promoting formation of dolomite as opposed to dissolution. This is in large part due to the fact that the pH is sufficiently high enough that the acidification term, R_1 is negligibly small. In fact, R_2 is only a factor of 4 larger than the pH independent dissolution rate (the R_3 term). The carbonatation term, R_2, was dominant over the acidification term (R_1) for all three waters.

The model of Pokrovsky and Schott (2001) (Equation 2.18) provides a negative dissolution rate (rate of precipitation) whenever the SI is positive (i.e. when $Q > K_{sp}$). Nearly all groundwater at the site with pH greater than 7.5 has SI > 0 with respect to dolomite. After pH adjustment to pH 6.5, it is likely

that SI will remain positive because of the increase in DIC resulting from sparging. Nonetheless, Pokrovsky and Schott's model was used to estimate the rate of dolomite dissolution after pH adjustment assuming a worst case scenario of far from equilibrium conditions (low SI). A rate of approximately 3×10^{-13} mol/cm^2-s was calculated for water from EW-4 after pH adjustment with CO_2 to pH 6.5. This rate is somewhat difficult to apply to field conditions because the dolomite surface area per unit volume is required. As a basis of comparison to the model of Busenberg and Plummer (1982) (Table 2-3), this rate is approximately equal to the pH independent rate R_3 and significantly less than the dominant dissolution terms (R_1 and R_2). The extremely slow rate of dissolution results from the moderate Ca^{2+} and moderate CO_3^{2-} concentrations that appear in the denominator of Equation 2.18.

2.3.2.3   Site Background pH Values

MW-506B is screened at the base of the Satilla and is a background well east southeast of the CBP. This well was measured to have a pH of 6.27 in 2010. Shallow Satilla wells to the northeast of the CBP (MW103C and MW104D) may be considered background and have an average pH of 6.1 (data collected in 2010). HWEast1, HWEast2 and HWEast3 are screened in the mid-Coosawhatchie A/B aquifer and have a pH of approximately 6.4. These wells provide a good indication of the background pH levels of the Satilla above the dolomitic sandstone and in the Coosawhatchie A/B below the dolomitic sandstone.

2.3.2.4   Summary

The lowering of the pH resulting from $CO_2(g)$ injection is not expected to influence the competency of the dolomitic sandstone aquitard for the following reasons:

- The target pH of the Proof of Concept test is 7.5, and the lowest the pH is expected to get is 6.5 because of the buffering imparted by HCO_3^-.
- Under current conditions, dolomite is saturated or supersaturated with respect to dolomite whenever the pH is greater than 7.5. Thus, dolomite dissolution is not expected to be thermodynamically favorable in locations where pH $\geq$ 7.5. Between pH 6.5 and 7.5 the saturation index varies between -3.0 and 1.8. Dissolution of dolomite is severely limited at saturation indices greater than -3 (Pokrovsky and Schott, 2001).
- The Busenberg and Plummer (1982) kinetic model predicts a negative dissolution rate (i.e. precipitation of dolomite) using post-sparge water chemistry for EW-4, EW-6 and EW-10.
- Dolomite dissolution rates are proportional to the H^+ raised to a stoichiometric power below pH 6.0. Rates of dolomite dissolution are insensitive to pH between pH 6 and 8 (Pokrovsky and Schott, 2001).
- CBP water has calcium concentrations of at least 1 mg/L. Pokrovsky and Schott (2001) have shown that dissolved calcium significantly inhibits dissolution rates at neutral pH for Ca^{2+} activities $> 10^{-4.5}$ (1.3 mg/L).

2.4 Evaluation of the Potential for Aquifer or Well Clogging Due to Solids Precipitation

2.4.1 Analysis Based Upon Laboratory Study

The proposed test location is in the area southeast of EW-11 (Figure 2-1). The closest existing monitoring wells in this location are MW-519A, MW-519B, and the MW-115 series. The water quality data for these wells are shown in Table 2-4 below.

Table 2-4: Water quality data (2010) in extraction and monitoring wells near the proposed Proof of Concept Test

Well	Total Alkalinity (mg/L as CaCO$_3$)	pH (field)	Dissolved silicon (mg/L as SiO$_2$)	Mercury (µg/L)	Sulfide (mg/L)	Chloride (mg/L)
EW-4	5,020	12.02	1,470	200	16.7	7,640
EW-6[a]	15,970	11.96	12,900	1,080	32.2	18,000
EW-10	3300	11.55	866	152	30.8	5150
EW-11[b]	5,001	11.74	2,270	172	37.5	15,000
MW-519A[c]	998	10.31	94.9	8.36	2.8	1,740
MW-519B[b]	7,410	11.90	3,200	163	25.2	25,100
MW-115B[c]	865	9.27	134	6.2	2.93	1,210
MW-115C[b]	5,800	11.85	2,870	136	27.6	17,100
MW-115D	2,137	10.19	345	13.8	29	12,600

(a) EW-6 is highlighted because of the distinct water quality encountered in this well.
(b) Screened in the Deep Satilla.
(c) Screened in the Mid Satilla.

The water quality in wells screened at the base of the Satilla near the proposed test have pH of approximately 11.8, total alkalinity of approximately 6,100 mg/L as CaCO$_3$ and dissolved silicon concentrations of 2,800 mg/L as SiO$_2$. Of the waters tested in the CO$_2$ laboratory test, these values are most similar to that of EW-4. In addition, the sulfuric acid demand of EW-11 (Figure 3-1), is only 15% less than that of EW-4.

The potential for well clogging during the Proof of Concept test appears to be minimal based upon results obtained from the CO$_2$ sparging laboratory study (Section 2.1). The study showed that sparging of EW-4 (medium acid demand) and EW-10 (low acid demand) to pH 6.5 did not result in significant solids generation. Long-term standing of CO$_2$-sparged water from EW-4 and EW-10 in separatory funnels for over 1 month showed no visual solids. It is expected that sparging in the proposed area near EW-11 will not produce significant solids because of the similar water quality to that of EW-4.

EW-6 did produce a significant amount of solids (Figure 2-6), and had a high TSS of 13.9 g/L after sparging with CO$_2$ to a pH of 6.7. Among the titration data collected by CH2M Hill (1997), EW-6 stands out for its extremely high acid demand and high dissolved silicon concentrations. The demand of EW-6 for sulfuric acid is more than two-times as high as EW-5 which ranks second in terms of demand (Figure 3-1), and is more than 3 times that of EW-11. The total alkalinity and dissolved silicon of EW-6 are much larger than EW-4 and EW-11. EW-6 therefore is distinct among the other waters in which acid demand was measured in the CO$_2$ laboratory testing and prior sulfuric acid titration testing.

12

EW-6 and MW-352B represent the highest dissolved silicon concentrations within the CBP (12,900 and 18,800 mg/L as SiO_2). These dissolved silicon concentrations are much greater than the surrounding areas. A probability plot of dissolved silicon concentrations for wells with pH > 10.5 is shown in Figure 2-9. Approximately 90% of all wells with pH > 10.5 have dissolved silicon concentrations less than 5,000 mg/L. Thus, the water quality of EW-6 with respect to dissolved silicon concentrations is not representative of the CBP as a whole.

The material formed after sparging EW-6 water with CO_2 was a gelatinous material that began to form once the pH dropped below approximately 7 (Figure 2-6). Figure 2-8 shows the general scheme for silica precipitation from Neville et al. (2012). In general, silica precipitation follows two distinct pathways depending upon the pH of the medium. Dissolved monomeric silicon ("hydrolyzed silane") begins to polymerize once it is supersaturated. This results in nucleation of small nanoparticulate silica clusters. Based upon the scheme shown in Figure 2-8 (Neville et al., 2012), these clusters can either form i) gelatinous silica if the pH is less than 7.0 or ii) colloidal silica of 0.2 to 2.0 μm in size if the pH is greater than 7.0. The pH is therefore very important to whether gelatinous silica gel or colloidal silica is formed. Gelatinous silica gel is a much more of a threat to well or aquifer clogging than colloidal silica.

Even for water with similar characteristics as EW-6, clogging is only expected to be an issue in locations where gelatinous silica is formed (i.e. where the pH drops below pH 7.0). During sparging, it is conceivable that the pH in areas closest to CO_2 gas channels will reach such a low pH. In these locations near EW-6, precipitation of gelatinous silica is expected. However, it would be extremely difficult to decrease the pH lower than 7.0 over a large volume of water because of the buffering imparted by the dissolved carbon dioxide (Figure 2-3). Effective pH neutralization without well clogging may be possible even in the area near EW-6 with the highest dissolved silicon concentrations if pH is maintained above 7.0.

2.4.2 Analysis Through the Proof of Concept Test

Pre- and post-sparging aquifer testing will be employed to assess whether any measurable reduction in aquifer hydraulic conductivity or pumping well specific capacity occurs as a result of the sparging. This testing and the analysis of the data are discussed in detail in Section 3.3

2.5 Analysis of Potential CBP Migration during Proof of Concept Test

Mounding of the groundwater table during in situ *air* sparging, is a well-recognized phenomenon. Similar mounding occurs with CO_2 sparging. However, mounding associated with either air or CO_2 sparging is a transient phenomenon. Mounding occurs as the air (or CO_2) expands into the saturated, porous media, creating a network of air (or CO_2) pathways or channels. Once the air channels reach the water table and break through to the vadose zone, the groundwater mound begins to decay and becomes negligible during steady-state operating conditions. An example of this behavior is illustrated in Figure 2-11(a), which is a case study by Lundegard (1995). At this site (Lundegard's Site 1) groundwater mounding of as much as 1.7 feet was observed at a distance of five feet from the sparge well. More distant wells evidenced progressively less mounding. In this example of continuous sparging, the mounding decayed rapidly after initiation of sparging reaching pre-sparge levels in two to four hours.

Studies have also shown that immediately following cessation of sparging, the water table collapses in the vicinity of the sparge well creating a similarly short-lived depression in the groundwater table. This phenomenon is illustrated in Figure 2-11(b) also from Lundegard (1995). At this site

13

(Lundegard's Site 2) groundwater mounding of 1.3 feet was observed at a distance of six feet from the sparge well. In this example of non-continuous sparging, the mounding decayed rapidly after initiation of sparging reaching pre-sparge levels in two to four hours. The sparging was then suspended at a time of 5.3 hours followed by a similarly short-lived depression in groundwater levels caused by partial collapse of the network of air channels in the saturated zone.

The case studies presented by Lundegard (1995) indicate that significant mounding occurred for only two to four hours after initiation of air sparging. The short-term nature of the mounding dictates that any lateral impact upon groundwater or plume migration will be quite small. In addition, the relatively short duration of CO_2 sparging versus the often long-term nature of air sparging means that the ensuing collapse of the groundwater mound into a groundwater depression following cessation of sparging will reverse much of the nominal lateral migration of the CBP during the proof of concept test.

As an illustration of the likely magnitude of lateral plume migration induced by a single well CO_2 sparge test, calculations have been performed based upon the observed transient mounding reported by Lundegard (1995) and Lundegard and LaBrecque (1995), coupled with the estimated hydraulic conductivity of 1×10^{-2} cm/sec (28.3 ft/day) and an effective porosity of 0.25 of the Satilla Formation at the Brunswick site estimated in the RI Addendum (GeoSyntec, 2002). The work of Lundegard and LaBrecque (1995) showed that the maximum mounding occurred rapidly after initiation of sparging and then declined quasi-linearly for two to four hours. The areal extent of the mounding varied from roughly 30 to 70 feet. In the calculations presented in Table 2-5, the average hydraulic gradient over the duration of mounding is taken to be one-half the maximum mounding, divided by the radial extent of the mounding. Separate calculations have been performed for mound durations of two and four hours. As the calculations illustrate, in most cases then transient mounding would induce groundwater in the vicinity of the air sparging well to migrate only a few tenths of a foot. In all scenarios, the migration is less than one foot. As revealed by Lundegard and LaBrecque (1995), cessation of sparging would result in a collapse of the water table producing a transient depression that would reverse much of the sparging-induced migration.

The calculations shown in Table 2-5 indicate that the extent of groundwater movement as a result of the mound caused by sparging is minimal (on the order of a few tenths of a foot). The longitudinal mixing induced by this movement can be estimated as well. The extent of dispersion is related to the length scale under consideration (Domenico and Schwartz, 1998). Field data from Gelhar et al. (1992) indicates that at scales of less than 1 m, longitudinal dispersivities are less than 10^{-2} m (0.0328 ft). Assuming a Fickian dispersion model, the length scale associated with mechanical mixing is equal to:

$$L_d = \sqrt{4D_L t} \qquad \text{where } D_L = \alpha_L v + D_m \qquad (2.20)$$

where D_L is the longitudinal dispersion, α_L is the longitudinal dispersivity, v is the groundwater velocity, and D_m is the molecular diffusion coefficient in water. An upper-bound groundwater velocity of 5.6 ft/d can be calculated for a mound height of 1.5 ft, and a radial extent of mounding of 30 ft. Assuming a worst case longitudinal dispersivity of 0.0328 ft, and a molecular diffusion coefficient of 9×10^{-5} ft²/d (1×10^{-6} cm²/s), the dispersion length scale for a 4 hour duration is only 0.34 ft. Thus, the extent of mixing will be extremely small.

14

Table 2-5
Calculated Extent of Groundwater
Migration Induced by CO_2 Sparging

Duration of Mounding = 2 hours

Radial Extent of Mounding	Maximum Mound Height in Feet			
	0.5	1	2	3
30	0.08	0.16	0.31	0.47
40	0.06	0.12	0.24	0.35
50	0.05	0.09	0.19	0.28
60	0.04	0.08	0.16	0.24
70	0.03	0.07	0.13	0.20

Duration of Mounding = 4 hours

Radial Extent of Mounding	Maximum Mound Height in Feet			
	0.5	1	2	3
30	0.16	0.31	0.63	0.94
40	0.12	0.24	0.47	0.71
50	0.09	0.19	0.38	0.57
60	0.08	0.16	0.31	0.47
70	0.07	0.13	0.27	0.40

K_h in ft/day = 28.3
Eff. Porosity = 0.25

In summary, the above analysis indicates that a single sparge well has a negligible effect on mobilization of groundwater or, in this case, the CBP. The mounding associated with air or CO_2 sparging is transient; rarely lasting more than a few hours after initiation of sparging and then recedes to pre-sparging levels. Moreover, after cessation of sparging, which is expected occur quite quickly in CO_2 sparging as opposed to the typically longer duration of air sparging, the water table collapses producing a transient depression that reverses much of the slight groundwater migration prompted by start-up of the CO_2 sparging. In a full-scale application, it is envisioned that CO_2 sparging could be sequenced across the sparge well field in such a way to similarly produce no appreciable migration of the surrounding groundwater.

2.6 Monitoring of CO_2 Off-Gassing and Worker Safety

The site Health and Safety Plan will be amended specifically to address the CO_2 injection testing activities. In general, continuous monitoring of oxygen in the breathing zone in the immediate vicinity of the injection well will be conducted to confirm safe working conditions. If oxygen levels drop below an approved concentration range, the injection testing will be stopped and the area will be evacuated until normal oxygen concentrations resume. In addition, it is anticipated that grab sample testing for mercury vapor and hydrogen sulfide will also be conducted at pre-approved intervals in the breathing zone. The

Health and Safety plan will dictate the appropriate response and protective equipment, as appropriate, in the event that mercury vapor and/or hydrogen sulfide vapor is detected in the breathing zone. It is anticipated that oxygen, carbon dioxide and hydrogen sulfide levels will be monitored with a standard multi-gas meter such as a BW GasAlert Micro5 MultiGas Monitor, or equal. Mercury vapor in the breathing zone will be monitored by a Jerome 413X Mercury Vapor Analyzer, or equal.

2.7 Evaluation of the Permanence of Mercury and other Metals Sequestration

The geochemical conceptual model for mercury within the CBP is discussed in the RI (GeoSyntec, 1997). E_h-pH diagrams were prepared for a representative "background water" and CBP water. The E_h-pH diagrams indicate that there is a transition from soluble mercury sulfide complexes (HgS_2^{2-}) to insoluble HgS(s) that occurs under moderately reducing conditions between pH 8.5 and 10.5.

Groundwater data was plotted on the diagram to shed light on the dominant forms of mercury as a function of E_h and pH. The highest Hg concentrations appear at the highest pH values. This is not surprising since they were both released to groundwater in the same general location. Background water at the site which has low to non-detect Hg plots in a region where the predominant species is HgS(s). This implies that low Hg concentrations are expected as the pH decreases to that of background water due to precipitation of mercury sulfide. The trend of the site groundwater E_h-pH composition from most-impacted toward background water roughly parallels the top and bottom boundaries of the HgS(s) and HgS_2^{2-} fields and intersects the HgS(s)/HgS_2^{2-} boundary near background conditions. Data from 2010 was plotted in a similar fashion and showed similar results (Figure 2-10).

There is evidence that decreasing the pH will result in a decrease in dissolved Hg concentrations. As pointed out in the RI (GeoSyntec, 1997), sulfide concentrations drop to near zero at the downgradient edge of the CBP, as defined by the sharp decrease in mercury concentration. On either side of this boundary, sulfide concentrations are elevated (due to the strongly reducing conditions of the ground water). This suggests that precipitation of mercury and other metal sulfides along the reaction-front at the downgradient edge of the caustic brine pool is consuming the aqueous sulfide. Beyond this reaction front there is essentially no dissolved mercury or other metals to precipitate as sulfides, and thus the sulfide concentrations are elevated. Similar plots created using the 2010 data for the deep Satilla wells also show a modest decrease in sulfide concentrations coincident with a drop in Hg which could be interpreted as a "sulfide reaction front."

In terms of stability of precipitated mercury, Barnett et al. (2001) measured oxidative dissolution rates of metacinnabar by O_2(aq) varying from 1.34 to 5.87 $\times 10^{-2}$ μmol/m^2-d (1.55 to 6.79 $\times 10^{-17}$ mol/m^2-s). The authors note that these rates are much slower than those considered stable in the environment such as quartz and feldspar, and that HgS(s) may be a viable long-term repository for Hg in the subsurface.

Speciation models have been developed by many authors for Hg complexes with reduced sulfur. In general, these models show that dissolved mercury concentrations decrease with decreasing pH in systems containing sulfides and polysulfides. For example, Jay et al. (2000) used a speciation model to describe total dissolved mercury concentrations as a function of pH in systems containing synthetic cinnabar and dissolved sulfide. The extent of the decrease in mercury concentrations with pH was dependent upon the total dissolved sulfide in the system and whether or not zero valent sulfur is present.

16

E$_h$-pH diagrams are useful and instructive in understanding geochemistry of trace metals such as mercury, however they often present an overly simplistic view of speciation. In reducing environments, mercury speciation is known to be dominated by (Skyllberg, 2008):

- Hg(II) complexes with sulfide such as $HgHS^-$, HgS_2^{2-}
- Hg(II) complexes with polysulfides such as $Hg(S_x)_2^{2-}$, HgS_xOH^-,
- Hg(II) complexes with thiol groups present on dissolved organic matter (DOM)
- HgS(s) precipitated as metacinnabar or cinnabar

Recent evidence has shown that DOM interacts strongly with metacinnabar effectively limiting particle growth thereby producing nanoparticulate HgS(s) that could be perceived as dissolved (Gerbig et al., 2011; Graham et al., 2012). Filter-passing Hg-S-DOM polynuclear clusters or HgS(s) nanoparticles stabilized by DOM may be the dominant forms of "dissolved mercury" in these systems. The complexities of Hg speciation in sulfidic systems make it very difficult to predict how changes in geochemical conditions will affect dissolved mercury conditions.

The Proof of Concept test is being designed to provide information about the extent to which dissolved mercury and other metal concentrations will change upon sparging with CO_2. As described in sections 3.7 and 3.8, groundwater from various monitoring wells will be sampled pre- and post-sparging for basic water chemistry (e.g. pH, TDS, alkalinity) dissolved metals (Hg, Cr, As), and geochemical parameters (ORP, sulfide, sulfate, ferrous iron), with the aim of understanding how sparging with CO_2 affects aquifer geochemistry and speciation of metals.

2.7.1 Effect of CO_2(g) on Metals Geochemistry

An additional concern of USEPA was that the injected CO_2 may interact with and affect the geochemistry of metals in the subsurface. CO_2 sparging imparts DIC (HCO_3^- and CO_3^{2-}) to the water and lowers the pH. However, injection of CO_2 will not directly interact with metals in the subsurface. Carbonate and bicarbonate are not strong ligands for Hg, As and Cr.

- Hg: Speciation is dominated by aqueous complexes with bisulfide (HS^-), polysulfides (HS_x^-), and thiol groups present in DOC (see above text).
- As: Speciation of As(III) and As(V) is dominated by aqueous complexes with bisulfide (HS^-), polysulfides (HS_x^-).
- Cr: For Cr(III), speciation is dominated by hydroxide ion and complexes with carboxylate and phenolic functional groups on DOC. For Cr(VI), speciation is dominated by $HCrO_4^-$, CrO_4^{2-}, and potentially chloro complexes.

17

3   PROOF OF CONCEPT TEST WORK PLAN

The objectives of the proof of concept test and the technical approach to achieving those objectives, while addressing the expressed concerns of USEPA and GEPD in connection with the 2010 Work Plan, have been set forth in Section 2. In Section 3, we describe the individual elements of the work plan.

3.1   Construction of Sparge Well and Additional Monitoring Wells

The proof of concept test would be conducted in the vicinity of EW-11, near existing well clusters MW-115 and MW-519, as depicted in Figure 3-1. This portion of the site was selected because it is generally representative of the CBP in terms of pH, acid demand, and mercury levels. It also has the aforementioned existing monitoring wells that can be used in the proof of concept test. It is proposed that two additional monitoring well clusters be constructed, with wells screened at the A, B, and C intervals (i.e. shallow, intermediate, and deep within the Satilla Sand formation); and one additional A interval well adjacent to EW-11. The vertical positioning of these proposed new monitoring wells and the existing wells is illustrated in Figure 3-2. which is a cross-section through the monitoring well network. The alignment of this geologic cross-section is given on Figure 3-1. Also shown on Figures 3-1 and 3-2 is the proposed sparging well, SW-1.

A screen length of 5 feet will be used for the sparge well and the monitoring wells. The sparge well will be constructed of 4-inch PVC and the monitoring wells will be constructed of 2-inch PVC. A typical well construction is shown in Figure 3-3.

Following installation, the wells will be developed to remove material which may have settled in and around the well screen. Development will consist of the removal of ten well volumes or achieving a turbidity reading of less than 50 NTUs. During this development, the approximate maximum yield and specific capacity of the well would be determined.

Drill cuttings and other investigation derived waste (IDW) will be temporarily drummed, labeled, transported, and staged at a waste accumulation area. IDW will be characterized and disposed at an appropriate off-site repository.

3.2   Site Surveying

The new injection well (SW-1) and new monitoring wells will be incorporated into the existing site survey. Ground and top-of-casing elevations will be recorded and incorporated into the existing site survey using known monuments and control locations.

3.3   Pre-Sparging Aquifer Testing

A 24-hour aquifer test will be conducted by pumping from well SW-1 at a rate determined from the yield testing described in Section 3.1. A 24 hour period is customary for this type of test. The main objective of the test is to define the transmissivity and by extension the hydraulic conductivity of the formation. The aquifer will probably behave as a water table (i.e. unconfined) aquifer. Water table aquifers typically exhibit three stages of drawdown behavior. Early-time behavior is characterized by rapid drawdown as the lower (pumped) portion of the aquifer initially behaves almost like a confined or semi-confined aquifer with a low storativity characteristic of such aquifers. The rapid initial rate of drawdown then slows due to delayed gravity drainage from the upper portion of the aquifer. During this

intermediate period, further drawdown may cease altogether in some observation wells. In the third and last phase, the aquifer begins to dewater and further drawdown becomes controlled by the specific yield of the aquifer. The transmissivity is best calculated from the early-time data (within the first few hours of the test) before delayed gravity drainage comes into play and the aquifer begins transitioning from a storativity-controlled early-time behavior to a late-time specific yield-controlled behavior. Thus, a 24-hour test will provide more than enough information to determine the aquifer's transmissivity and hydraulic conductivity. For our purposes, even a 4-hour test would likely generate sufficient data. However, having the full 24-hour data set will enhance our understanding of overall aquifer behavior, which may have future utility. The aquifer testing program will include antecedent data collection, a constant rate aquifer (pumping) test and associated data collection, and recovery (post aquifer test) data collection. Every effort will be made to schedule the test during a period when precipitation is not anticipated. Each phase of the study is described below.

3.3.1 Data Collection

Groundwater levels, barometric pressure, tidal stage, and precipitation will be monitored during the antecedent, aquifer test, and recovery period. The methodologies for each of these data collection efforts are described below:

Groundwater Levels

After the data loggers are deployed as described below, and during the three day antecedent data collection period, a manual round of water levels will be collected from each well. Groundwater levels within the wells listed in Table 3-1 will be recorded throughout the aquifer testing program by means of automatic data loggers, with occasional manual water level measurements for quality assurance/quality control and data backup. Solinst Level Loggers (or equivalent) will be employed for automatic data logging. The data logger will be set at a designated depth (the same depth throughout the aquifer testing program) within the well and securely affixed to prevent any movement. The short term pump/yield test results (Section 3.2) will be used to estimate the anticipated drawdown at each location and the pressure transducer at that location will be set approximately five feet below the maximum anticipated drawdown. The automatic data loggers will be synchronized for time and will be programmed to record antecedent water levels at 30-second intervals during the three-day antecedent monitoring period, the 24-hour aquifer test, and the 24 hour recovery period. A single laptop computer would be used to synchronize each of the data loggers to the computer's internal clock. In this manner, the data loggers will be time synchronized to the nearest one second. The data loggers will be deployed at the wells listed below and a manual water level measurement will be collected. The depth to water and time of collection will be recorded in the field book.

Table 3-1	
Transducer Installations	
Well/Well Cluster	No of Transducers
SW-1	1
MW-1A, B, C	3
MW-2A,B,C	3
MW-519A, B	2
MW-115A,B,C	3
MW-3A	1
EW-11	1
Tide Gage	1
Total	15

Barometric Pressure

Barometric pressure data will be collected by means of a Solinst barologger (or equivalent) programmed to record time and barometric pressure at the same intervals as the data loggers. The barologger would be suspended well above the static water level in one of the monitoring wells. Barometric pressure can be measured anywhere as long as the meter can equilibrate with the atmosphere. The monitoring well will be vented and therefore the pressure inside the well will have equilibrated with the barometric pressure. Locating the barologger in the well will also prevent it from being disturbed.

Precipitation

Precipitation will be monitored using an on-site rain gauge. Every effort should be made to schedule the test during a period when precipitation is not anticipated.

Tidal Stage

A tide gage will be placed at the confluence of Purvis Creek and the LCP ditch on the south side of the causeway. The tide gage would consist of a small diameter PVC pipe affixed to an existing piling or to a steel stake driven into the sediment bed. A Solinst datalogger would be mounted in the PVC pipe in the same manner as described for the monitoring wells.

Following the aquifer test and the monitoring of aquifer recovery, the data loggers will be removed from the wells and downloaded to a laptop computer.

3.3.2 Aquifer Test Well Pumping and Water Management

Pumping for aquifer test shall be performed using an adequately sized submersible pump. A submersible pump capable of pumping 10 gpm at design head will be selected for the pump tests. Power to the pump shall be provided by temporary on site generators. The discharge line shall be equipped with a check valve to prevent backflow into the well and a flow measuring and a throttling valve to measure and maintain the required flow rate identified during the yield test as described in Section 3.1. The discharge piping from the test pump shall be routed to the existing treatment facility. The piping options shall be either a temporary on-ground pipeline or temporarily tapping into the closest existing extraction well pipeline. Assuming a 10 gpm maximum potential yield capacity for a 24-hour test duration, the

maximum volume of water collected shall be approximately 14,400 gallons. The water shall be collected in the existing 17,000-gallon dual wall influent equalization tank. The water shall be either treated and reinjected into the aquifer (as currently approved) subsequent to aquifer test completion or shall be sent to an offsite treatment facility. Both pre and post sparging aquifer pump test water shall be handled in similar fashion. If subsequent calculations or site conditions indicate the requirement for a greater pump test storage volume, arrangements for the use of mobile tank(s) will be made.

3.3.3 Data Analysis

The collected data will first be analyzed to make appropriate corrections to the drawdown and recovery data as necessary, based on barometric pressure fluctuations during the course of the test, water level trends in the aquifer, tidal stage fluctuations, or precipitation-induced water level fluctuations. The necessity of barometric pressure corrections will depend upon the degree of barometric pressure fluctuation during the course of the aquifer test and the extent to which monitoring wells exhibit barometric efficiency. The barometric efficiency of monitoring wells will be determined from the antecedent water level data. Similarly, the necessity of tidal stage corrections will depend upon the extent to which monitoring wells exhibit tidal efficiency and tidal lag times. The barometric efficiency and associated tidal time lag of monitoring wells will be determined from the antecedent water level data. If significant water level trends exist in the aquifer prior to start of the aquifer test, corrections may also be necessary to account for these non-pumping related water level changes.

Precipitation events during the course of an aquifer test can be more problematic. Ideally, the aquifer tests would be scheduled for a time when precipitation events are not forecast. Precipitation events can be difficult to compensate for as precipitation can affect aquifer water levels in significant and non-uniform ways. Consequently, a significant precipitation event may be cause for postponement or termination of an aquifer test. This will be a decision made by the supervising hydrogeologist depending upon the severity with which the precipitation event effects groundwater level data collection.

The corrected drawdown data would initially be analyzed qualitatively to gain a general sense of aquifer behavior. This analysis would be followed by conventional time-drawdown analysis of wells screened in the pumped hydrostratigraphic zone. If, as expected, the aquifer behaves as an unconfined aquifer, the Neuman time-drawdown method would be employed (Neuman, 1975) to calculate aquifer transmissivity, hydraulic conductivity, storativity during early-time behavior, late-time specific yield, and vertical anisotropy. Drawdown in the pumped zone at the conclusion of the pumping test would also be analyzed by means of the Cooper-Jacob distance-drawdown method (Cooper and Jacob, 1946) or the DeGlee method (De Glee, 1930; Kruseman and DeRiddler, 1991) depending upon aquifer characteristics to determine transmissivity, hydraulic conductivity, and specific yield. These distance-drawdown methods also permit extrapolation of drawdown in the aquifer to the pumping well. The extrapolated drawdown in the aquifer at the pumping well can then be compared to the *measured* drawdown in the pumping well, which includes well losses, to calculate pumping well efficiency. This will allow determination of whether the well efficiency appreciably changes after CO_2 sparging (when the aquifer testing is repeated).

3.4 Pre-Injection Monitoring

Analysis of pH, specific conductivity (SC), dissolved oxygen (DO), temperature, oxidation-reduction potential (ORP) and specific gravity (using a hydrometer) will be performed in the field and

recorded in the sampling log book. A suitable analytical laboratory will be used for analysis of lab pH, dissolved inorganic carbon, alkalinity, total organic carbon, total dissolved solids, dissolved silicon, chloride and TAL metals (which includes Ag, Al, As, Ba, Be, Ca, Cd, Co, Cr, Cu, Fe, Hg, K, Mg, Mn, Na, Ni, Pb, Sb, Se, Tl, V, and Zn). The following geochemical parameters will also be measured: ferrous iron, sulfate, and dissolved sulfide.

3.5 Temporary Injection Equipment Design and Set-up

A temporary carbon dioxide sparge system shall be installed near SW-1 during the pilot test. A typical process flow diagram for the carbon dioxide sparge system is shown in Figure 3-4. The following options for carbon dioxide supply shall be considered and will be dependent on final carbon dioxide demand calculations.

1) Individual liquefied CO_2 cylinders (for low CO_2 requirement < 1000 lbs) or
2) Manifolded liquefied CO_2 cylinder pack (for medium CO_2 requirement 1000 – 5000 lbs) or
3) Vendor supplied flat bed truck containing liquefied carbon dioxide gas and vaporizers (for high CO_2 requirement > 5000lbs)

In each case, the liquefied CO_2 delivery system would be a vendor-provided system and would include an integral vaporizer and interconnecting piping. Instrumentation on the sparge line shall include flow, temperature and pressure indication. The sparge line shall contain needle valves and pressure regulating valve to optimize flow and pressure as necessary during the pilot tests. The system shall include a pressure relief valve set to relieve at appropriate setpoint to prevent over pressurization of the system and to protect the well formation. A separate tracer gas (sulfur hexafluoride) cylinder shall be connected to the sparge line. The tracer gas line shall have a dedicated pressure regulator and needle valve to bleed in gas at required rate and pressure. All operation on the sparge system shall be manual. Electrical power source may be required for refrigeration of bulk CO_2 tank which would be provided by onsite generators.

3.6 CO₂ Sparging

CO_2 sparging would be conducted in much the same manner as biosparging. In biosparging, the objective is to deliver oxygen into the saturated zone to promote biodegradation of target organic compounds. In contrast, air sparging often has as its principal objective the stripping of volatile organic compounds from the aqueous phase into the sparged air, which can then be collected from the vadose zone and treated ex situ. Aerobic biodegradation of organic compounds is typically a secondary objective of air sparging. Consequently, air sparging systems are often run continuously at high air flow rates to promote rapid stripping of volatile organic compounds from the aquifer. In biosparging systems, air is more commonly intermittently sparged into the aquifer only in sufficient quantities to match the oxygen demands of the biological reactions being stimulated in the aquifer. In biosparging, oxygen levels are often continuously monitored. When oxygen declines to a predetermined level, sparging is resumed for a short period of time to reestablish the air-filled channels and allow diffusion and advective mixing to bring oxygen back up to suitably high levels. This type of "pulsed injection" is continued until biodegradation objectives are met. In addition, oxygen transfer can potentially be more efficient under pulsed conditions because trapped air left in the aquifer continues to transfer oxygen to the groundwater in-between injection cycles.

22

Building upon the experience gained from biosparging applications, the CO_2 sparging proof of concept test would employ a pulsed CO_2 injection approach coupled with continuous monitoring of pH in the aquifer. In this way, we can better control the reduction in aquifer pH to target levels and increase the efficiency of CO_2 delivery to the aquifer. Careful pulsed CO_2 injection will also further avoid the potential of "overshooting" the target pH, although this potentiality is inherently minimized by the self-buffering effect of the carbonate produced by CO_2 reacting with water (See Section 2.1). The planned approach to pulsed injection during the proof of concept test is laid out in Table 3-2.

Table 3-2
Planned Sequence of Pulsed Sparging

Day	Planned Approach
Day 1 through 21	Sparge for 10 hours each day, followed by monitoring for 14 hours. Sparging would occur on weekdays, with weekends used for longer term monitoring of pH reductions occurring during a two-day non-sparging period
Days 21-28 ·	Monitoring

The above planned sequencing of CO_2 sparging and monitoring would be subject to adjustment on a daily or even more frequent basis depending upon the observed performance of the proof of concept test. Once target pH levels have been attained and have stabilized within a certain ROI, whether that occurs after one day, 14 days, or longer, active sparging would cease and continuous monitoring of any pH rebound would continue through Day 28. If pH reduction is not deemed to be occurring at a sufficient rate, the pulsing frequency might be adjusted to promote more advective mixing and diffusion of CO_2 into the aquifer. Increased pulsing might entail alternately sparging for one hour and resting for one hour for a total of ten hours each day.

3.6.1 CO_2 Sparging Calculations

Laboratory titrations of CBP water with 98% sulfuric acid (18.2 mol/L) performed by CH2MHill (Figure 3-5) indicate that the theoretical demand is approximately 2.0 gallons H_2SO_4 per 1000 gallons of water. This is estimated to bring the pH down to 7.5. Note that EW-6 has a much higher demand than the other waters, and it was therefore not used to estimate the demand. Since H_2SO_4 is a strong acid, it is capable of neutralizing two equivalents of base. The demand for H^+ is 272 equivalents per 1000 gallons of groundwater:

$$\left(\frac{2.0 \text{ gal } H_2SO_4}{1000 \text{ gal GW}}\right)\left(\frac{18 \text{ mol } H_2SO_4}{L}\right)\left(\frac{2 \text{ eq } H^+}{1 \text{ mol } H_2SO_4}\right)\left(\frac{3.785 \text{ L}}{1 \text{ gal}}\right) = \left(\frac{272 \text{ eq } H^+}{1000 \text{ gal GW}}\right) \quad (3.1)$$

CO_2 is a weak acid, and its ability to neutralize base depends upon the pH of the water. To translate H_2SO_4 demand to CO_2 demand, a prototypical CBP water was numerically titrated with both acids. The numerical titration was performed assuming all of the alkalinity (Alk) of the water is present as carbonate, silicate ions and hydroxide ion:

$$\text{Alk} = [HCO_3^-] + 2[CO_3^{2-}] + [Si(OH)_3^-] + 2[Si(OH)_2^{2-}] + [OH^-] - [H^+] \quad (3.2)$$

23

For the H_2SO_4 titration the alkalinity was decreased step-wise while holding DIC constant. For the CO_2 titration, the total inorganic carbon was increased stepwise while holding alkalinity constant. In both cases, the pH was calculated at each step.

EW-4 was selected as the prototypical water. Data collected from the laboratory study (Section 2.1) was used for the initial pH, alkalinity and total dissolved silicon. The results of the numerical titration (Figure 3-6) show that H_2SO_4 and CO_2 are equally effective in lowering the pH to 10. As the pH decreases below 10, CO_2 is only capable of donating 1 equivalent of H^+, and is therefore not as effective as H_2SO_4. At pH 7.5 (the target pH of the Proof of Concept Test), approximately 2-times as much CO_2 is required on a mole basis.

Taking into account the weak acid nature of H_2CO_3, the comparable demand for $CO_2(g)$ is 12,000 g CO_2 per 1,000 gallons of water (26.5 lbs per 1,000 gallons water).

$$\left(\frac{2.0\ gal\ H_2SO_4}{1000\ gal\ GW}\right)\left(\frac{18\ mol\ H_2SO_4}{L}\right)\left(\frac{2\ mol\ H_2CO_3}{1\ mol\ H_2SO_4}\right)\left(\frac{3.785\ L}{1\ gal}\right)\left(\frac{44\ g\ CO_2}{1\ mol\ H_2CO_3}\right)=\left(\frac{12,000\ g\ CO_2}{1000\ gal\ GW}\right) \quad (3.3)$$

These calculations assume 100% gas transfer to the water. Assuming a 15-ft ROI, 45 foot-thick saturated zone, and porosity of 0.30, one pore volume within the injection zone contains approximately 71,400 gallons of groundwater. At 100 percent CO_2 transfer, approximately 1,890 pounds of $CO_2(g)$ would be required for brine neutralization to pH 7.5. Assuming 10 percent efficiency, at least 18,900 lbs of CO_2 is required (10 times greater than theoretical demand).

The target flow rate for the test is 20 scfm. This flow rate was selected based upon guidance from ESTCP (Leeson et al., 2002), USEPA (2004) and the Army Core of Engineers Design Manual (2008). Additionally, the CO_2 case study described earlier used flow rates that bracketed 20 scfm. Assuming 20 scfm is attainable, the estimated duration of sparging to satisfy the CO_2 demand is 138 continuous hours assuming an efficiency of 10 percent. Since the sparging is scheduled for 10 hour intervals, theoretically, the target pH will be reached within 14 sparging cycles (14 days). If the transfer efficiency is considerably lower, and additional CO_2 is required, the proposed 14 day sparging cycle can be continued if monitoring results indicate that this would be beneficial. Conversely, if the ROI or true CO_2 demand is considerably smaller, then the number of sparge cycles can be decreased accordingly.

3.6.2 Use of SF_6 as a Tracer

The purpose of using sulfur hexafluoride (SF_6) as a tracer is to determine the vertical and lateral extent of CO_2 distribution in the target treatment zone. A small amount of SF_6 is blended into the CO_2 stream. As the CO_2/SF_6 mixture flows through gas channels in the aquifer, both gases will partition into groundwater and move away from the air channel-groundwater interface through the combination of diffusion, dispersion and advection (Leeson et al., 2002). SF_6 is commonly used as a tracer for air sparging studies because it does not occur naturally and background concentrations are extremely low. For example surface waters in equilibrium with current atmospheric SF_6 levels (6.9 pptv) have approximately 0.24 ng/L of dissolved SF_6. Also SF_6 can be detected at extremely low concentrations in water and is not biodegradable, so it acts as a conservative tracer to show where the injected gas was delivered.

24

During the injection, $SF_6(g)$ will be blended into the CO_2 stream whenever sparging is occurring. A small SF_6 cylinder holding at least 10 lbs of SF_6 will be connected to the CO_2 injection manifold as shown in Figure 3-4. A flow meter will be used to monitor and ensure proper SF_6 delivery. A back-pressure valve will be used to adjust the tracer gas pressure at the flow meter to at least 15 psig above the pressure in the CO_2 line to minimize effects of air injection line pressure fluctuations on the tracer delivery rate.

The maximum concentration of SF_6 is required to assess the percent saturation of groundwater samples collected after sparging. Therefore a baseline water sample containing saturated $SF_6(aq)$ will be collected during sparging start-up. A slip-stream valve on the air injection manifold will be used to bubble the CO_2/SF_6 gas stream vigorously through a 40 mL VOA vial containing initially tracer-free water for 2 minutes. This will saturate the water with SF_6. This sample will be analyzed as discussed in Section 3.8.

The SF_6 delivery flow rate was chosen by considering the desired maximum concentrations of SF_6 imparted to groundwater and the expected detection limit of SF_6. SF_6 concentrations are often measured via head space injection into a gas chromatograph with an electron capture detector (GC-ECD). The GC-ECD method is capable of measuring very low concentrations down to 10 pptv. The following is adapted from (Leeson et al., 2002):

$$Q_{SF_6} = Q_{tot} H C_{max.HS}\left(\frac{V_{HS}}{V_w}\right) \times 10^{-9} \tag{3.4}$$

where H is the Henry's law constant for SF_6 equal to 170 L water / L gas from Wilhelm et al. (1977), Q_{tot} is the total gas flow (in scfm), Q_{SF6} is the flow of SF_6 (in scfm), $C_{max.HS}$ is the maximum concentration of SF_6 in the headspace (in ppbv), V_{HS} is the head space volume and V_w is the volume of water sample subjected to analysis. The maximum head space concentration needs to be significantly higher than the GC-ECD detection limit to permit analysis of collected groundwater samples. A value of 20 ppbv was chosen for this test which is approximately 2000-times the detection limit. Assuming that the laboratory will use 1 mL of groundwater sample (V_w) with a 39 mL headspace for the extraction (V_{HS}), the design flow rate of SF_6 is 0.0027 scfm. This represents 0.013 % (v/v) of the total composition of the sparge gas. At the flow rate of 0.0027 scfm for the 137 hour sparging duration, a total of 3.8 kg (8.4 lb) of SF_6 is required for the test.

At the end of the sparging period, groundwater samples will be collected and analyzed for SF_6. In terms of data analysis, we will use the following methodology adapted from from Bruce et al (2001). In general, concentrations of SF_6 observed in groundwater samples can be broken up into three groupings: i) values approaching saturation (e.g., >40% of theoretical solubility) which indicate that the sample location lies within the "zone of aeration" of the air sparging system; ii) samples containing low concentrations of SF_6 (e.g., <10%) which indicate that an air channel may be in the vicinity of the sampling location (e.g., it may be within the "zone of treatment"), and iii) samples that have no SF_6 and are outside of the "zone of treatment."

3.7   Monitoring During CO_2 Injection

3.7.1   Groundwater Quality

Groundwater pH will be continuously monitored during the proof of concept test in each of the 13 monitoring wells using AquiStar TempHion Submersible Smart pH sensors with data logging capabilities, or equivalent. These sensors would be pre-programmed to collect data at 10 minute intervals and will be calibrated prior to installation. A connector cable allows downloading of collected data to a computer at any time during the test. The downloaded data is easily exported to spreadsheets or databases for analysis.

3.7.2 CO_2 Pressure and Flow Rate

The carbon dioxide sparge system shall be designed to deliver gas at a design rate of 20 scfm at 60 psi (i.e. up to approximately 2 times the well static head). Pressure regulators and flow control valve shall be used to maintain and optimize pressure and flow rates during pilot testing.

3.7.3   Groundwater Levels

Groundwater levels within the wells listed in Table 3-1 will be recorded throughout the aquifer testing program by means of automatic data loggers. Solinst Level Loggers (or equivalent) will be employed for automatic data logging. The data logger will be set at a designated depth (the same depth throughout the aquifer testing program) within the well and securely affixed to prevent any movement. The automatic data loggers will be synchronized for time and will be programmed to record water levels at five minute intervals during the CO_2 sparging period and for one day after conclusion of the sparging. A single laptop computer would be used to synchronize each of the data loggers to the computer's internal clock. In this manner, the data loggers will be time synchronized to the nearest one second. The data loggers will be deployed at the wells in Table 3-1 and a manual water level measurement will be collected. The manual depth to water measurement and time of collection will be recorded in a field book. The Solinst data loggers will be removed 24 hours after conclusion of the sparging period. If the aquifer water levels do not return to pre-sparge conditions within 24 hours, the data loggers will remain in place for an additional 6 days or until the mound recedes, whichever is shorter.

3.8   Post-Injection Monitoring

After the period of post- sparging monitoring is completed, the pH data loggers will be removed and the groundwater monitoring wells will be sampled. Analysis of pH, specific conductivity (SC), dissolved oxygen (DO), temperature, oxidation-reduction potential (ORP), and specific gravity (using a hydrometer) will be performed in the field and recorded in the sampling log book. A suitable analytical laboratory will be used for analysis of lab pH, dissolved inorganic carbon, alkalinity, total organic carbon, total dissolved solids, dissolved silicon, chloride and TAL metals (which includes Ag, Al, As, Ba, Be, Ca, Cd, Co, Cr, Cu, Fe, Hg, K, Mg, Mn, Na, Ni, Pb, Sb, Se, Tl, V, and Zn). The following geochemical parameters will also be measured: ferrous iron, sulfate, and dissolved sulfide. These monitoring efforts will provide useful information on the heterogeneity of CBP geochemistry after the sparging is completed sand will aid in the design of a full-scale treatment system. Samples for SF_6 will be collected in 40 mL VOA vials from all 13 monitoring wells. They will be sent to a suitable commercial laboratory specializing in SF_6 analysis.

Five out of 13 monitoring wells will be selected for rebound monitoring pending the outcome of pH and geochemistry results from the post-sparging sampling round. These wells will be sampled after 3

months and 6 months following conclusion of the sparge test to assess any rebound in pH and other constituents of concern. If no rebound is evidenced after six months, it is considered unlikely that significant rebound will occur thereafter. In any case, if the proof of concept test is considered successful and full-scale implementation is proposed, it would be preceded by a baseline round of analyses for the same parameters which would serve as a de facto third set of rebound measurements.

3.9 Post-Sparging Aquifer Testing

The post-sparging aquifer testing will follow the identical procedures set forth in Section 3.3

3.10 Health and Safety Plan

All work would be conducted in accordance with a health and safety plan as described in Section 2.6.

4   DATA EVALUATION AND REPORTING

In the proceeding sections, we describe the technical approach and specific procedures for implementation of the CO_2 sparging test. Before, during, and after the CO_2 sparging test, multiple measurements of a variety of parameters will be made to address the test objectives set forth in Section 2. This section discusses how these measurements will be evaluated and reported. After completion of the CO_2 Sparging Proof of Concept Test results will be reported in a Technical Report to USEPA that contains all the data collected and reported plus interpretive conclusions.

4.1   Radius of Influence
The radius of influence will primarily be determined based upon the measured changes in pH in the groundwater monitoring well network resulting from the CO_2 sparging test. However, other changes in geochemistry and metals content would also be reported and mapped. Figures will be prepared showing pre- and post-sparging levels of pH and other chemical parameters. These figures would include both plan and cross-section views.

4.2   Rate of Reaction
The rate of pH change in monitoring wells will be determined through in well datalogger pH monitoring during the CO_2 sparging test. Figures showing time series graphs of pH vs. time in key monitoring wells will be prepared.

4.3 CO_2 Sparge Efficiency
The efficiency of the CO_2 sparge proof of concept test will be assessed by means of a CO_2 mass balance. The mass of CO_2 injected will be compared to the mass of carbonic acid and other reaction products in the aquifer water. The differential between the CO_2 mass injected and the CO_2 accounted for in the reaction products will be considered to be the CO_2 escaping through the vadose zone to the atmosphere. The efficiency will be defined as the mass of CO_2 reacting with the CBP water divided by the total mass of CO_2 injected.

4.4   Reduction in Hydraulic Conductivity
As described in Section 3, aquifer testing would be conducted before and after the CO_2 sparging proof of concept test. Aquifer testing, rather than slug testing, as proposed in the 2010, was selected because aquifer testing provides a better measure of the hydraulic conductivity changes within the full radius of influence of the CO_2 sparging test. In contrast, slug tests provide a permeability measure within a limited region around each observation well. The specific procedures for aquifer testing and interpretation of the aquifer test data are given in Section 3 and will not be repeated herein. However, the results of the pre- and post-aquifer testing will be carefully compared to each other to discern any material changes in hydraulic conductivity. Figures exhibiting flow-normalized drawdown over time and distance-drawdown curves will be produced as part of this evaluation.

4.5   Reductions in Specific Capacity and Efficiency of the Aquifer Test Extraction Well
The specific capacity of the extraction well would be monitored during both the pre- and post-sparging aquifer test. Specific capacity is defined as the well's pumping rate divided by the observed drawdown in the well. This is typically expressed as gallons per minute per foot of drawdown. In addition, the efficiency of the extraction well would also be defined both during the pre- and post-aquifer

testing. Well efficiency is defined as actual drawdown in the aquifer adjacent to the extraction well divided by the observed drawdown in the well, itself, expressed as a percentage. The difference between observed drawdown in the aquifer and observed drawdown in the extraction well is due to well losses associated with groundwater passing through the sand pack and well screen. Any diminution in the hydraulic conductivity of the sand pack or the well screen due to clogging of precipitates would be reflected in a lower well efficiency and greater well losses.

4.6 Changes in Geochemistry within the Radius of Influence

Changes in the CBP geochemistry within the cone of influence would be measured pre- and post-CO_2 sparging. Key parameters such as pH would also be measured during the sparge test. This data would be analyzed by preparing trilinear diagrams of major ion geochemistry, ratio plots, and/or graphs of other water quality constituents over time.

4.7 Extent of Groundwater Mounding

The transducer data would be analyzed to define the vertical magnitude, radial extent, rate of propagation, and life cycle of mounding associated with the CO_2 sparging test. The monitoring would be continued throughout the sparging test and for 24 hours afterward to monitor the final transient mounding, the recession to a steady state level, and the collapse and formation of a depression in groundwater levels following cessation of the test. Figures showing the extent of mounding in the cross section at various times during and after the CO_2 sparging test would be prepared to illustrate the life cycle of mounding and subsequent depression in groundwater levels.

4.8 Determine Practical CO_2 Injection Rates

Following the conclusion of the CO_2 sparging test and monitoring of water level collapse, the CO_2 injection rate would be increased to evaluate the maximum feasible injection rates without creating pressures in the formation that could induce hydraulic fracturing.

4.9 Monitoring pH and Chemical Constituent Rebound Following the CO_2 Sparging Test

The groundwater monitoring well network will be monitored immediately following the completion of the CO_2 sparging proof of concept test and then after three months and six months following the test. This data will allow for evaluation of any rebound in pH or other key constituents such as mercury. It should be noted that some rebound is expected since the sparge test should produce a localized decrease of pH within its radius of influence. Subsequent to the test, natural gradients in the aquifer will cause the area of circumneutral pH to gradually move downgradient and simultaneously allow higher pH CBP water to gradually migrate into the test zone from upgradient. Time series graphs of pH, mercury and other constituents will be prepared to illustrate any changes in these parameters over time.

29

5   PROPOSED WORK SCHEDULE

The schedule for implementation of the CO_2 sparging proof of concept is given in Figure 5-1. It is anticipated that the actual field work entail approximately 13 weeks from receipt of approval to proceed. The report of the proof of concept test would be completed within 10 weeks after completion of the post-injection monitoring. Subsequent brief reports would be prepared providing the results of the three and six month rebound monitoring.

6 REFERENCES

Barnett, M.O., Turner, R.R., Singer, P.C., 2001. Oxidative dissolution of metacinnabar (β-HgS) by dissolved oxygen. Appl. Geochem. 16, 1499-1512.

Bruce, C.L., Amerson, I.L., Johnson, R.L., Johnson, P.C., 2001. Use of an SF6-Based Diagnostic Tool for Assessing Air Distributions and Oxygen Transfer Rates during IAS Operation. Bioremediation Journal 5, 337-347.

Busenberg, E., Plummer, L.N., 1982. The kinetics of dissolution of dolomite in CO_2-H_2O systems at 1.5 to 65 degrees C and 0 to 1 atm PCO_2. Am. J. Sci. 282, 45-78.

Busenberg, E., Plummer, L.N., 1986. A comparative study of the dissolution and crystal growth kinetics of calcite and aragonite, in: Mumpton, F.A. (Ed.), Studies in Diagenesis. USGS, pp. 139–168.

CH2M Hill, 2010. Draft Pilot Test Work Plan Caustic Brine Pool In-situ Treatment LCP Chemicals Site, Brunswick, GA.

Chou, L., Garrels, R.M., Wollast, R., 1989. Comparative study of the kinetics and mechanisms of dissolution of carbonate minerals. Chem. Geol. 78, 269-282.

Cooper, H.H., Jacob, C.E., 1946. A Generalized Graphical Method for Evaluation Formation Constants and Summarizing Well-Field History. Transactions, American Geophysical Union 27, 526-534.

De Glee, G.J., 1930. Over Groundwaterstromingen Bij Wateronttrekking Door Middel Van Putten. Delft, the Netherlands, p. 175.

Gelhar, L.W., Welty, C., Rehfeldt, K.R., 1992. A critical review of data on field-scale dispersion in aquifers. Water Resour. Res. 28, 1955-1974.

GeoSyntec, 2002. Groundwater RI Addendum Report LCP Chemicals Brunswick, Georgia.

Gerbig, C.A., Kim, C.S., Stegemeier, J.P., Ryan, J.N., Aiken, G.R., 2011. Formation of Nanocolloidal Metacinnabar in Mercury-DOM-Sulfide Systems. Environ. Sci. Technol. 45, 9180-9187.

Graham, A.M., Aiken, G.R., Gilmour, C.C., 2012. Dissolved Organic Matter Enhances Microbial Mercury Methylation Under Sulfidic Conditions. Environ. Sci. Technol. 46, 2715-2723.

Jay, J.A., Morel, F.M.M., Hemond, H.F., 2000. Mercury Speciation in the Presence of Polysulfides. Environ. Sci. Technol. 34, 2196-2200.

Kharaka, Y.K., Thordsen, J.J., Kakouros, E., Ambats, G., Herkelrath, W.N., Beers, S.R., Birkholzer, J.T., Apps, J.A., Spycher, N.F., Zheng, L.E., Trautz, R.C., Rauch, H.W., Gullickson, K.S., 2010. Changes in the chemistry of shallow groundwater related to the 2008 injection of CO2 at the ZERT field site, Bozeman, Montana. Environ. Earth Sci. 60, 273-284.

Kruseman, G.P., DeRiddler, N.A., 1991. Analysis and Evaluation of Pumping Test Data, second edition. International Institute for Land Reclamation and Improvement, p. 377.

Leeson, A., P.C., J., R.L., J., Vogel, C.M., Hinchee, R.E., Marley, M., Peargin, T., Bruce, C.L., Amerson, I.L., Coonfare, C.T., Gillespie, R.P., McWhorter, D.B., 2002. Air Sparging Design Paradigm. Environmental Security Technology Certification Program (ESCTP).

Lundegard, P.D., 1995. Air Sparging: Much Ado About Mounding, in: Hinchee, R.E. (Ed.), In Situ Aeration: Air Sparging, Bioventing, and Related Remediation Processes. Battelle Press, Columbus, OH, pp. 21-30.

Lundegard, P.D., LaBrecque, D., 1995. Air Sparging in a Sandy Aquifer (Florence, Orgeon, U.S.A.): Actual and Apparent Radius of Influence. J. Contam. Hydrol. 19, 1-27.

Martell, A.E., Smith, R.M., Motekaitis, R.J., 2004. NIST Critically Selected Stability Constants of Metal Complexes, 8.0 ed. NIST.

Morse, J.W., Arvidson, R.S., 2002. The dissolution kinetics of major sedimentary carbonate minerals. Earth-Science Reviews 58, 51-84.

Neuman, S.P., 1975. Effect of Partial Penetration on Flow in Unconfined Aquifers Considering Delayed Gravity Response. Water Resources Research 11, 329-342.

Neville, F., Mohd. Zin, A., Jameson, G.J., Wanless, E.J., 2012. Preparation and Characterization of Colloidal Silica Particles under Mild Conditions. J. Chem. Ed.

Plummer, L.N., Wigley, T.M.L., Parkhurst, D.L., 1978. The kinetics of calcite dissolution in CO_2-water systems at 5 degrees to 60 degrees C and 0.0 to 1.0 atm CO_2. Am. J. Sci. 278, 179-216.

Pokrovsky, O.S., Schott, J., 2001. Kinetics and Mechanism of Dolomite Dissolution in Neutral to Alkaline Solutions Revisited. Am. J. Sci. 301, 597-626.

Pokrovsky, O.S., Schott, J., Thomas, F., 1999. Dolomite surface speciation and reactivity in aquatic systems. Geochim. Cosmochim. Acta 63, 3133-3143.

Skyllberg, U., 2008. Competition among thiols and inorganic sulfides and polysulfides for Hg and MeHg in wetland soils and sediments under suboxic conditions: Illumination of controversies and implications for MeHg net production. J. Geophys. Res. 113, G00C03.

U.S. Army Corps of Engineers, 2008. Engineering and Design: In-Situ Air Sparging. Department of the Army, Washington, DC.

USEPA, 2004. How to Evaluate Alternative Cleanup Technologies for Underground Storage Tank Sites: A Guide for Corrective Action Plan Reviewers.

Wilhelm, E., Battino, R., Wilcock, R.J., 1977. Low-pressure solubility of gases in liquid water. Chem. Rev. 77, 219-262.

Figure 2-1

CBP and Extraction Well System

Mutch Associates, LLC
Environmental Engineers and Scientists
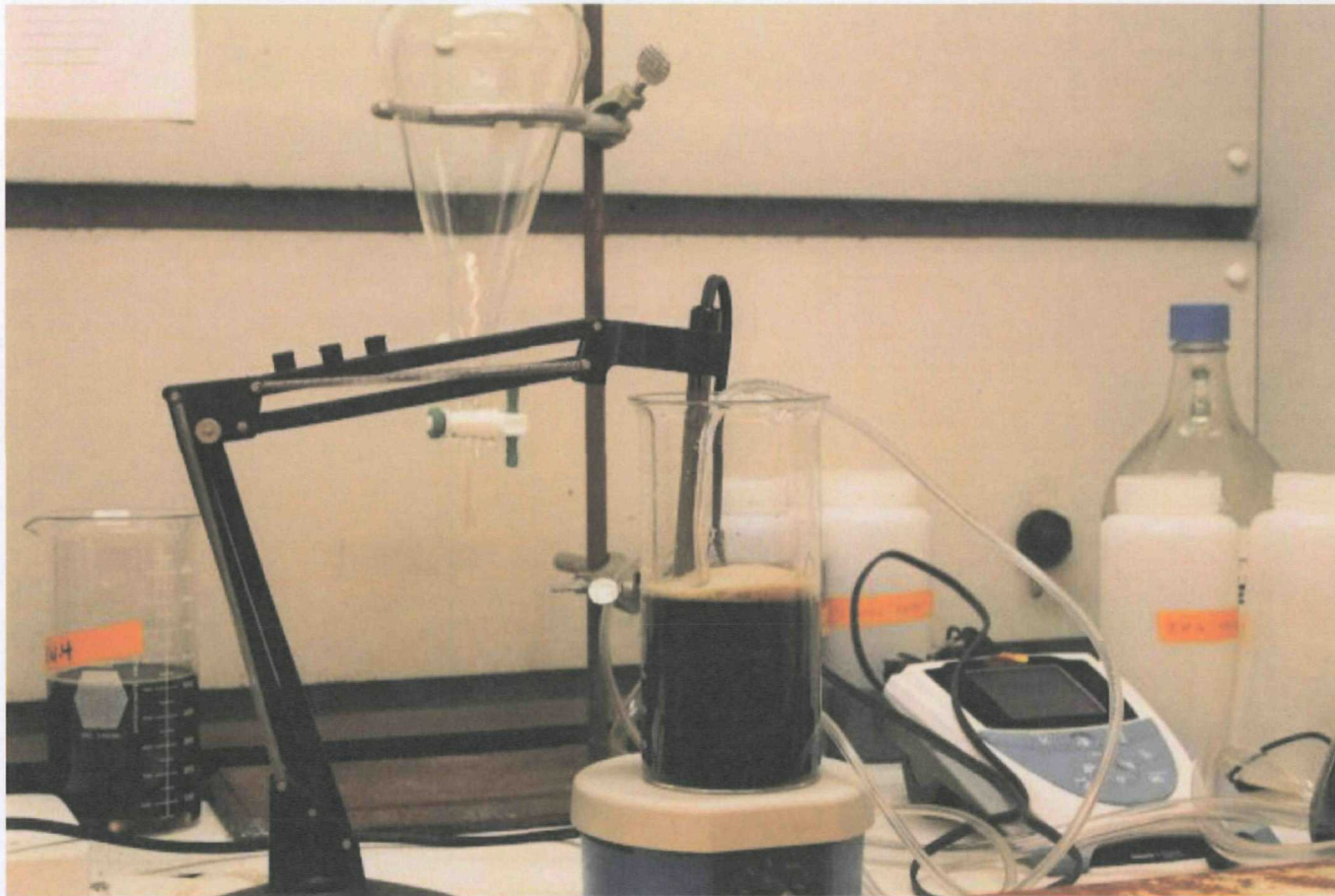
Figure 2-2

Experimental Set-Up for $CO_2(g)$
Lab Sparging Test

Mutch Associates, LLC
Environmental Engineers and Scientists
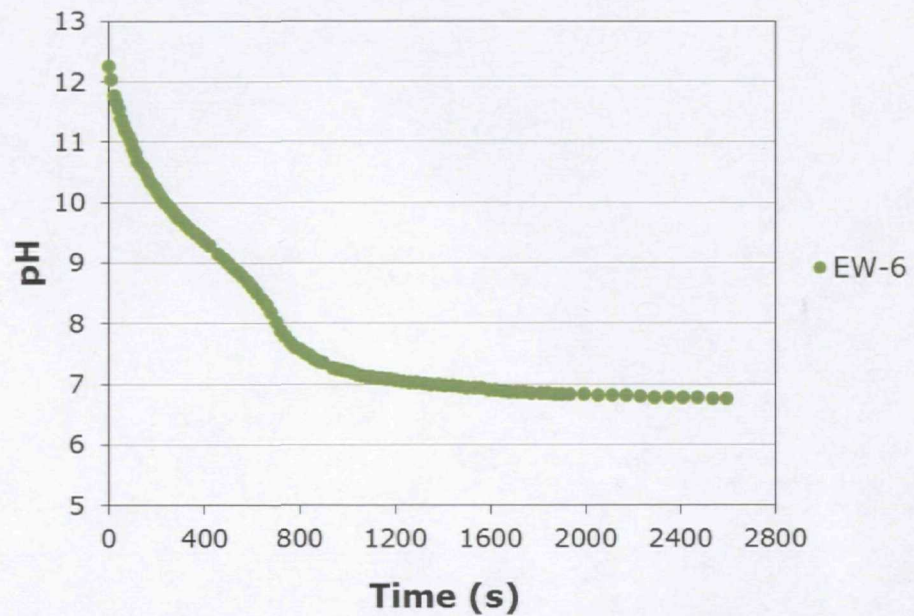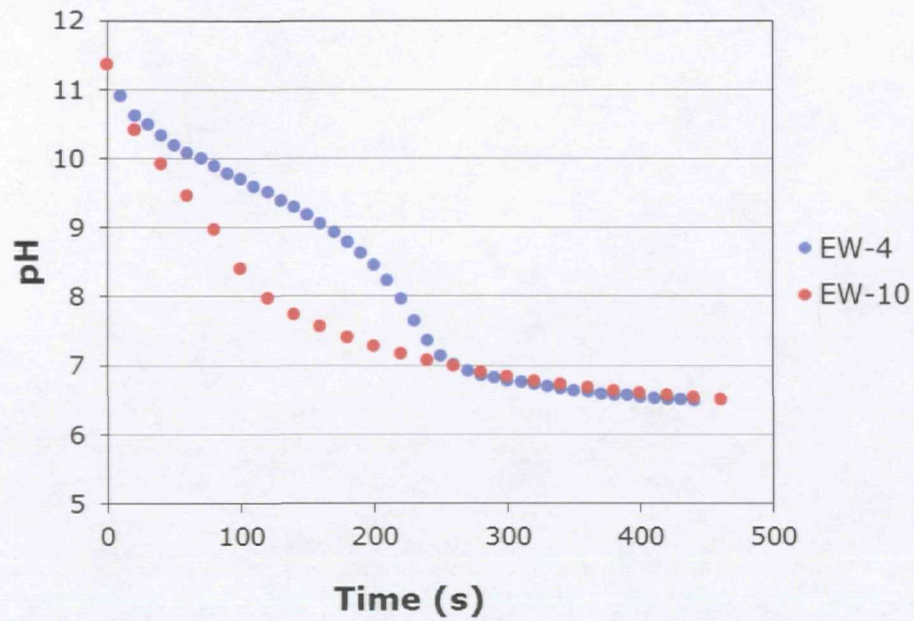
Figure 2-3

Titration Curves
pH versus Sparging Time

Mutch Associates, LLC
Environmental Engineers and Scientists
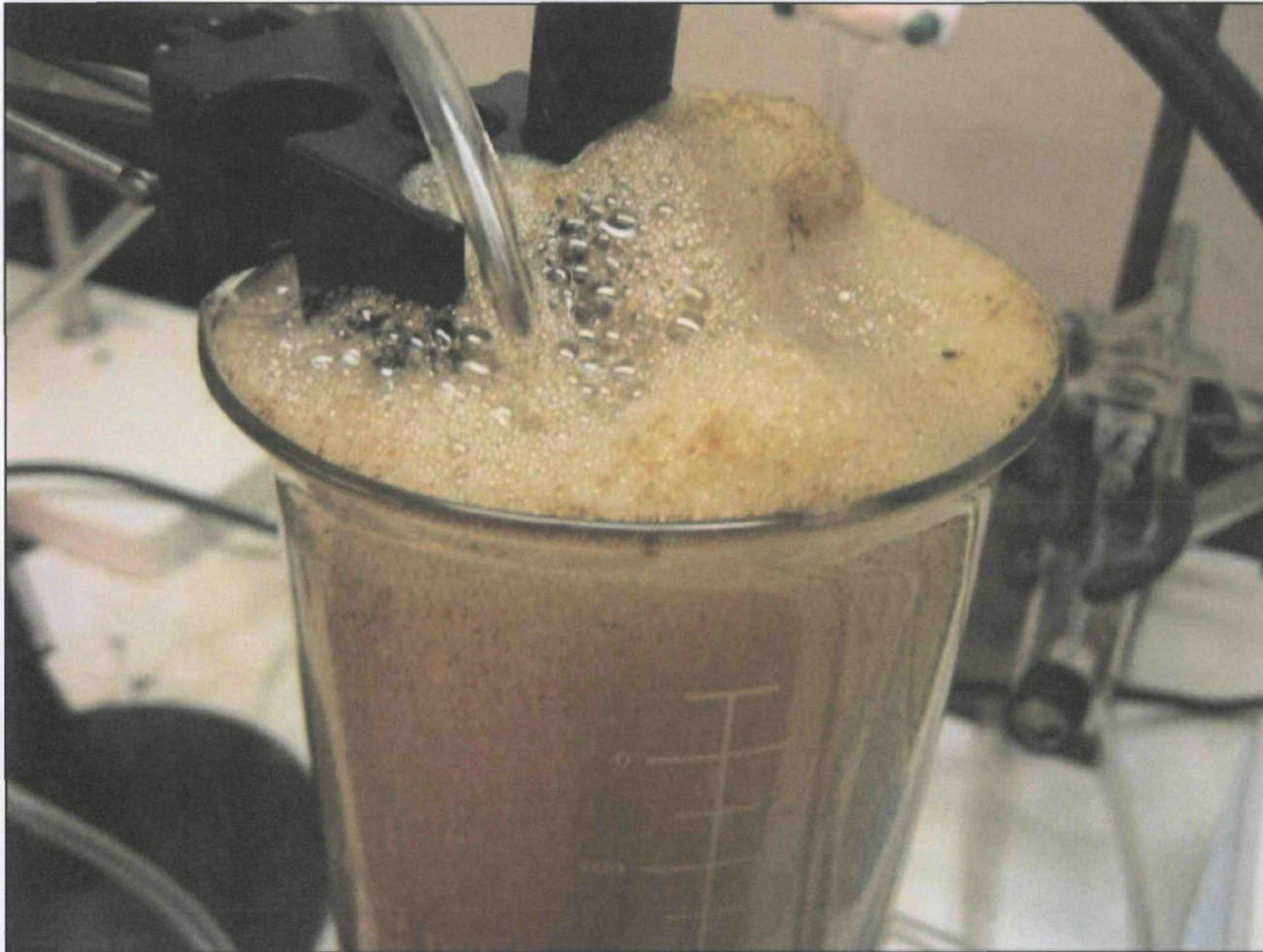
Figure 2-4

Photo of Foaming that Resulted from Continual CO_2 Sparging

Mutch Associates, LLC
Environmental Engineers and Scientists
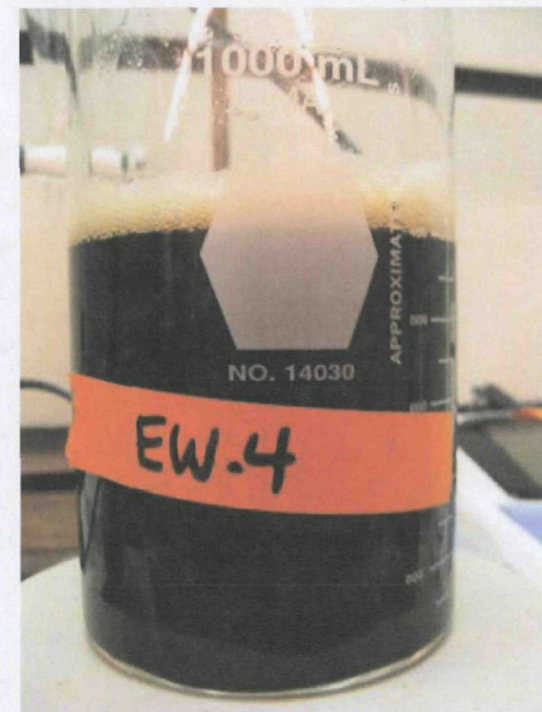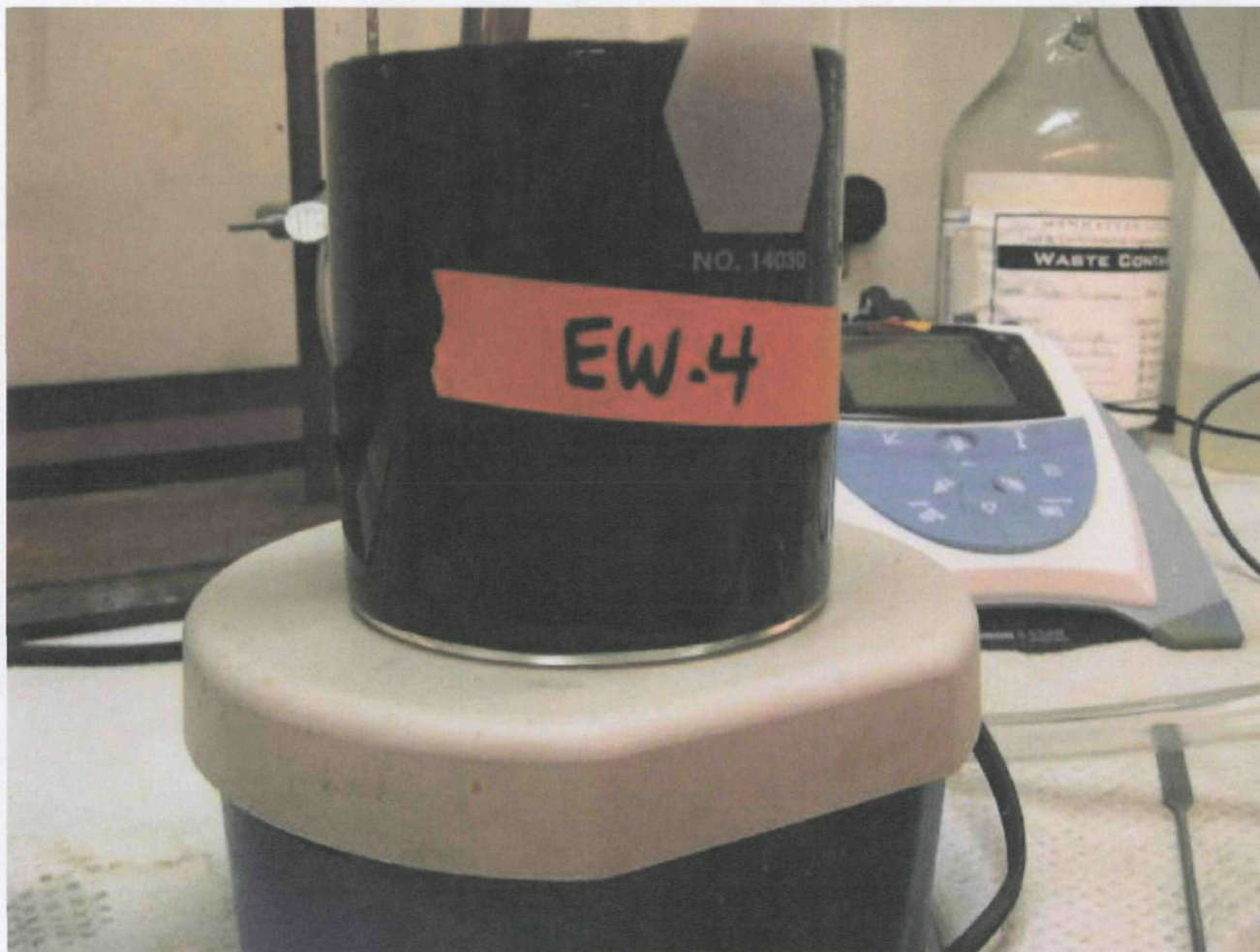
Figure 2-5

No Visual Evidence of Solids

Mutch Associates, LLC
Environmental Engineers and Scientists

Figure 2-6

EW-6 Gelatinous Material
at pH <7

Mutch Associates, LLC
Environmental Engineers and Scientists
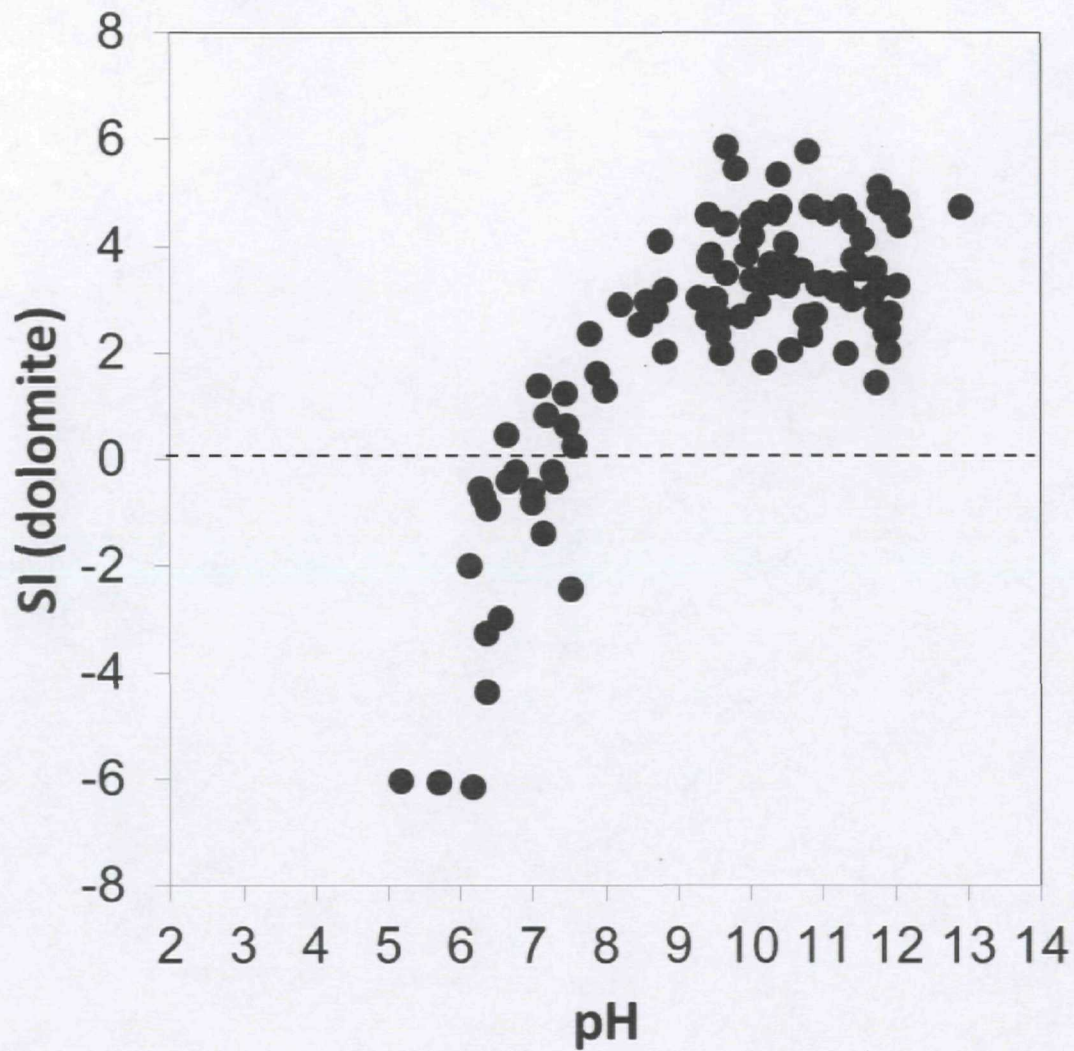
Figure 2-7

SI for Dolomite versus pH
(May/June 2010 Data)

Mutch Associates, LLC
Environmental Engineers and Scientists

OH
|
HO—Si—OH hydrolyzed silane
|
OH

polymerization

nucleation
1–5 nm

gelling

growth
5–200 nm

pH < 7

pH = 7–10

silica gel

colloidal silica

0.2–2 μm
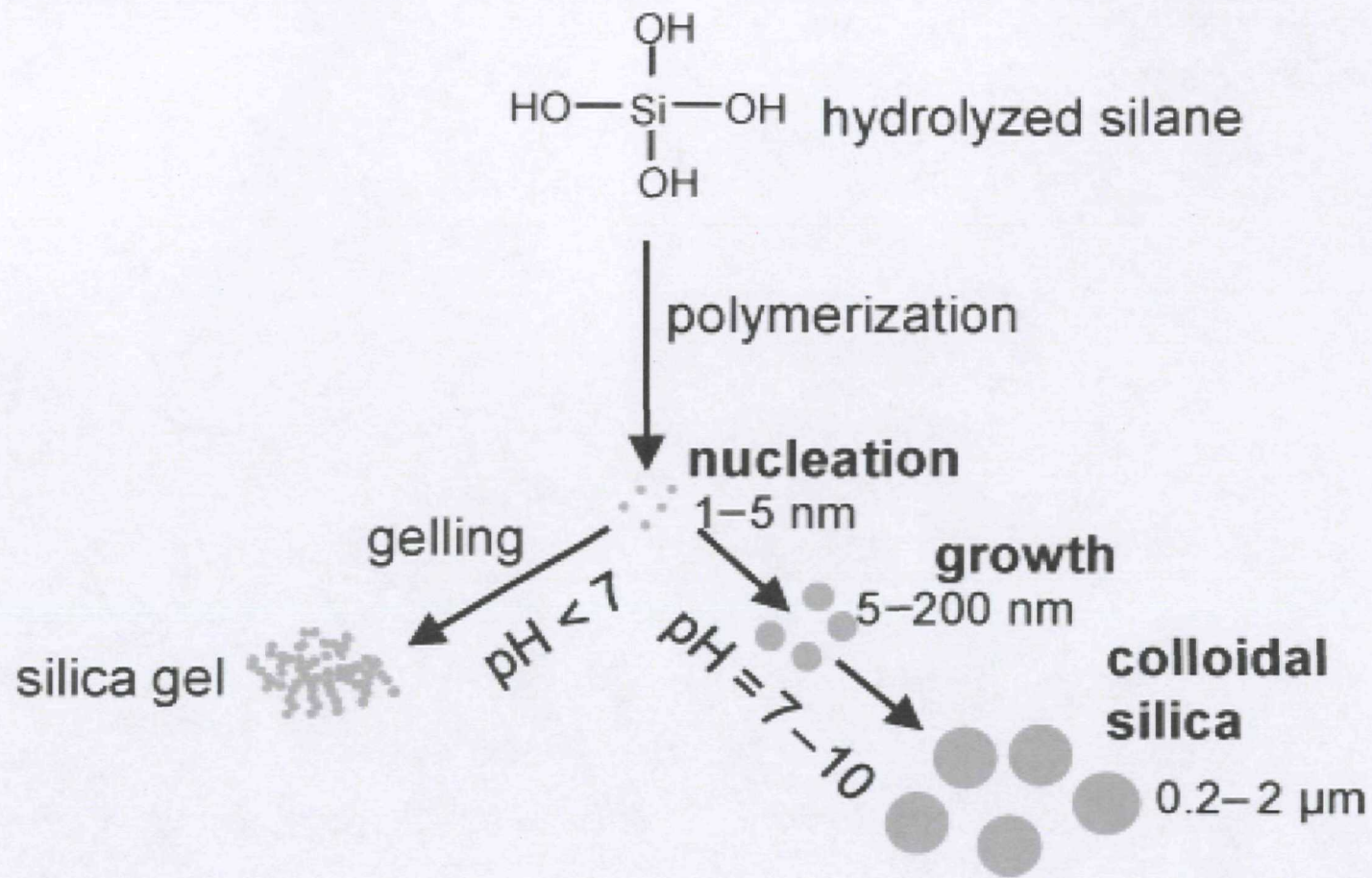
Figure 2-8

Silica Precipitation Scheme
at Various Solution pH

Mutch Associates, LLC
Environmental Engineers and Scientists

From Neville et al. (2012)
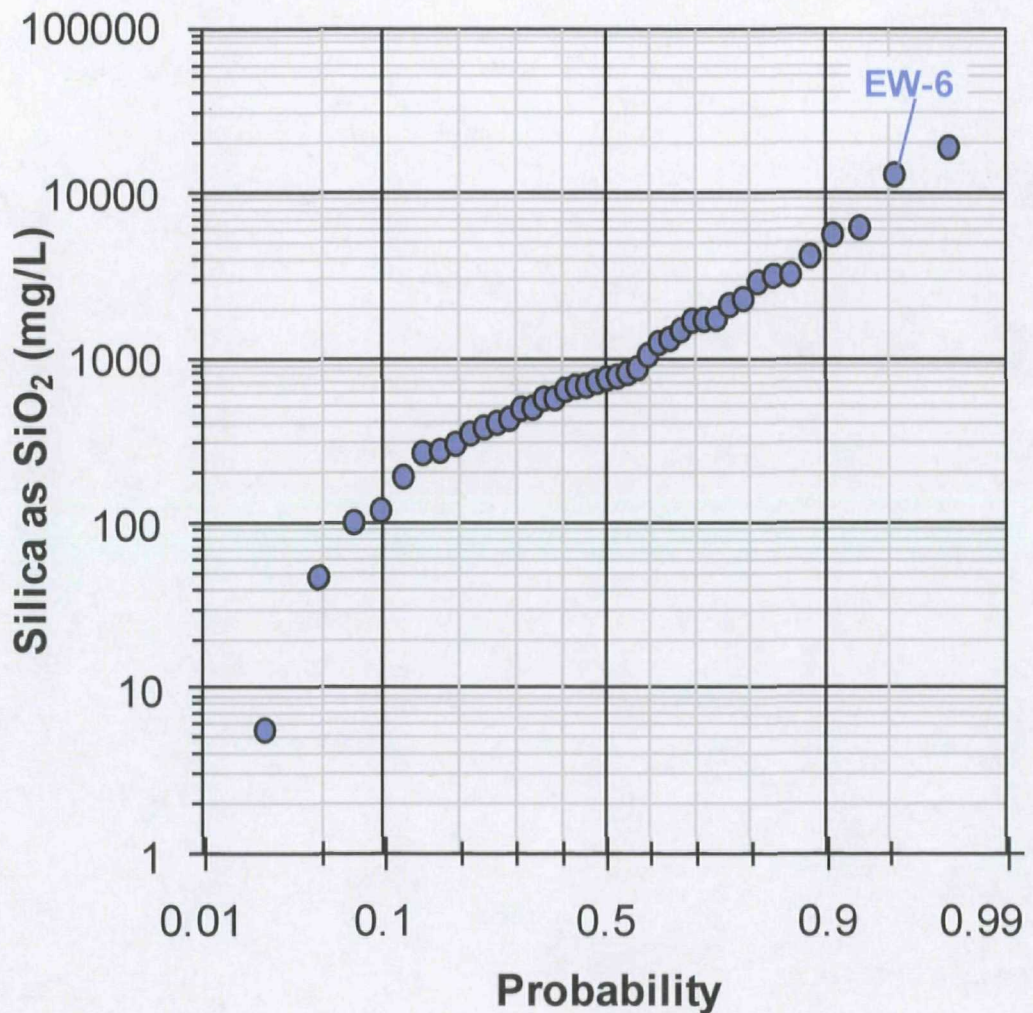
Figure 2-9

Probability Plot of Silica
Concentrations for Wells
with pH> 10.5

Mutch Associates, LLC
Environmental Engineers and Scientists
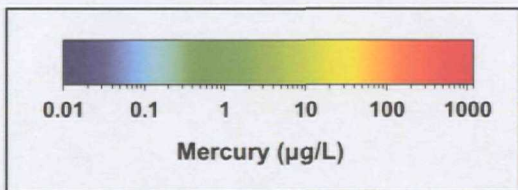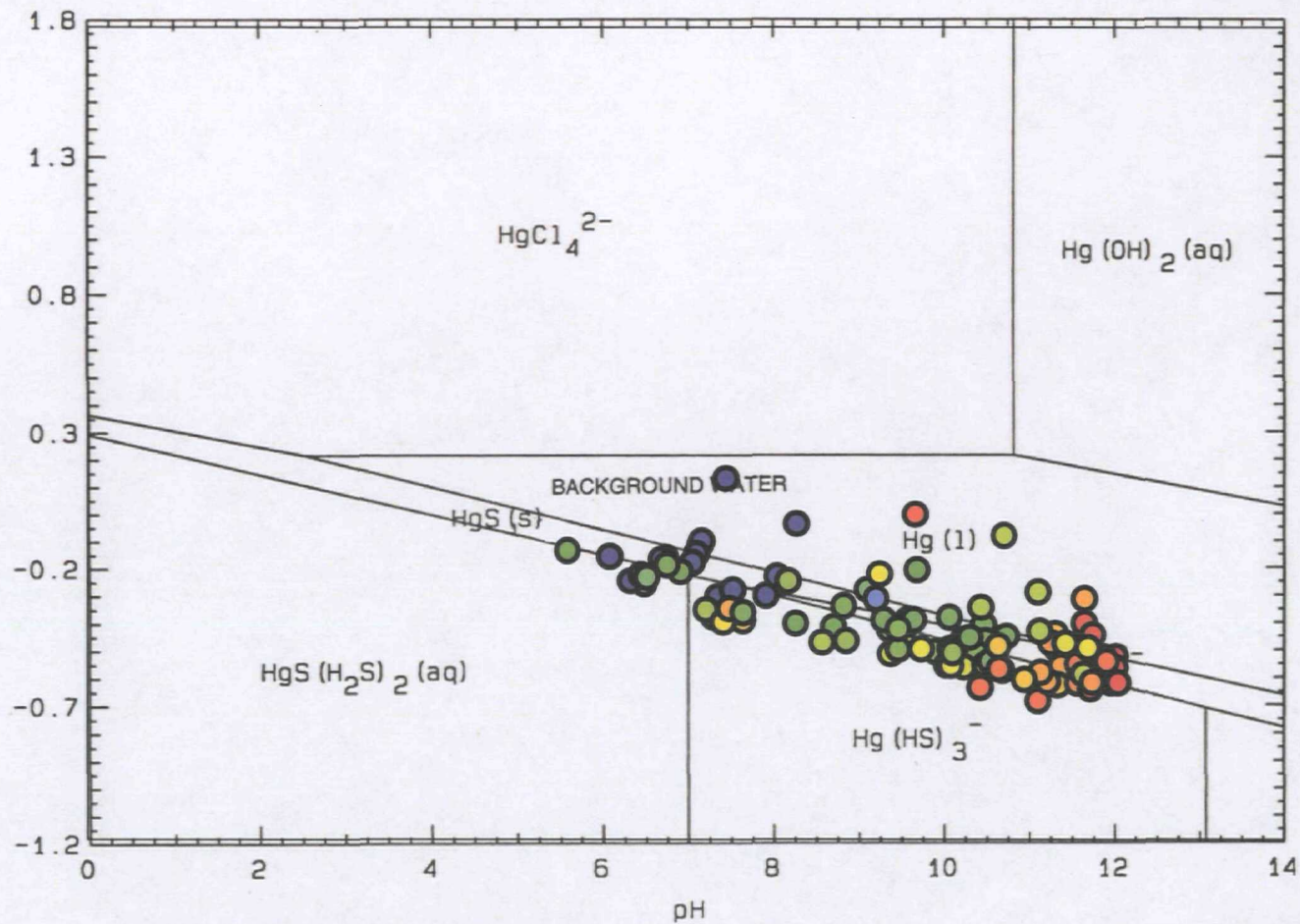
Figure 2-10
Mercury Concentrations (2010)
plotted on E_h-pH diagram
from RI (GeoSyntec, 1997)

Mutch Associates, LLC
Environmental Engineers and Scientists
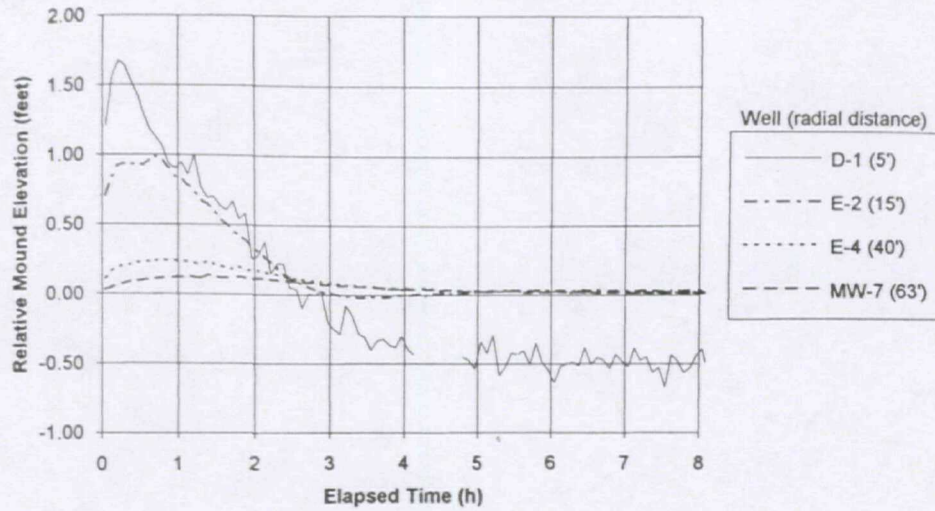
(a) Plot of mounding versus elapsed sparge time at Site 1. The rapid rise to a peak followed by a gradual decrease towards presparging levels is the typical transient response observed at most sites. Legend shows radial distance from sparge well to observation well. D-1 transducer removed from well between 4.2 and 4.7 h.

(From Lundegard, 1995)
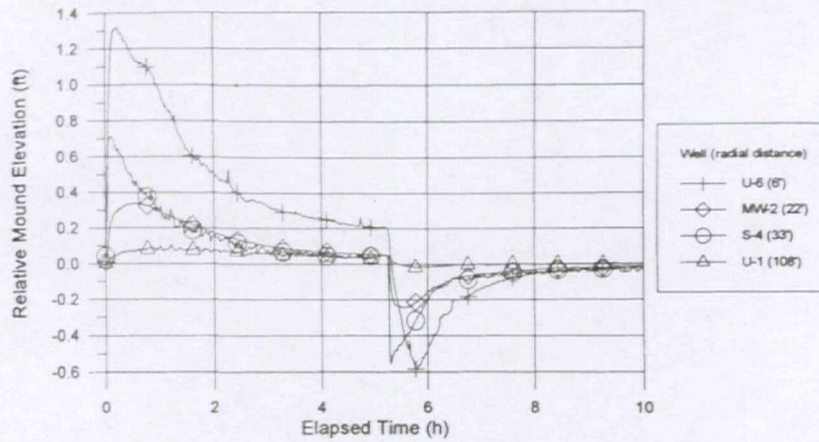
(b) Plot of mounding versus elapsed sparge time at Site 2. Note the magnitude of mounding is greater 33 ft (10 m) from the sparge well than it is at 22 ft (6.7 m) from the sparge well. This anomaly suggests heterogeneity in the saturated zone.

(From Lundegard, 1995)

Figure 2-11

Examples of Transient Water Level Responses to Air Sparging

Mutch Associates, LLC

Environmental Engineers and Scientists

VICINITY MAP

Proof of
Concept
Test
Area

MW-517B
MW-517A

PZ-4
PZ-4

PZ-10 PZ-10

A

EW-11
MW-3A

MW-519B
MW-519A   MW-1A,B,C
SW-1   MW-115D

MW-2A,B,C
MW-115C
A'

MW-115B   MW-115A

1 inch = 25 feet
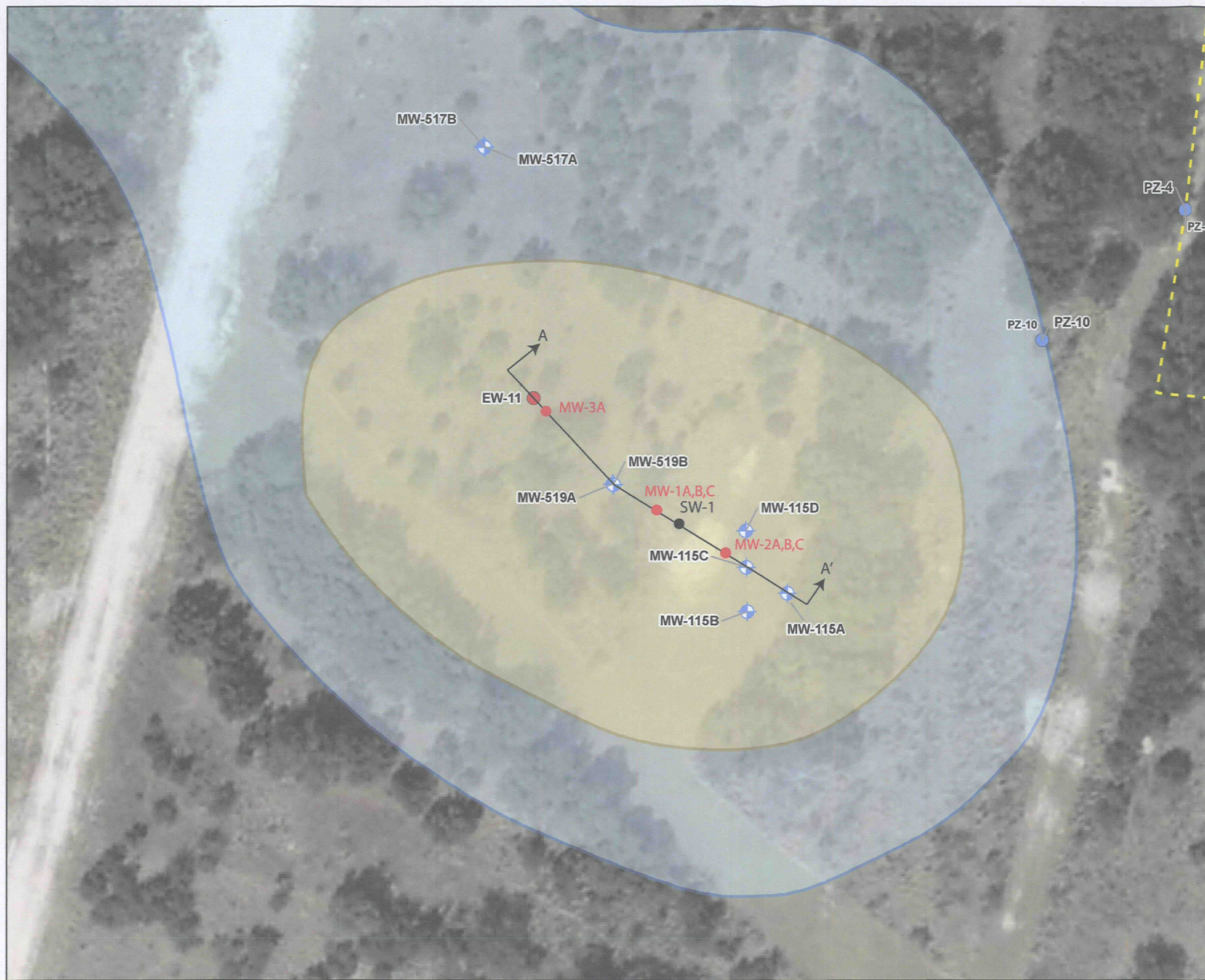
LEGEND

● Existing Extraction Well

⬦ Existing Monitoring Well

● Existing Piezometer

MW-1A, B, C
● Proposed Monitoring Well or Well Cluster

SW-1
● Proposed Sparge Well

– – Infiltration Galleries

Caustic Brine Pool (pH > 11.5)

Caustic Brine Pool (pH > 10.5)

N

0   25   50
          Feet
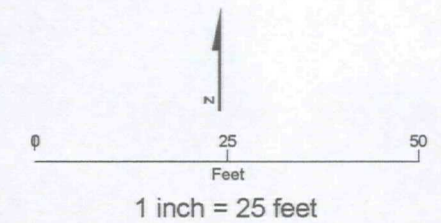
Note:
The approximate current lateral extent of the CBP in the
Upper Surficial Aquifer is based primarily on the most recent
comprehensive data set from 2007 and supplemented with
more recent data collected from extraction wells and
500-series monitoring wells between 2009 and April 2010.

Figure 3-1

Plan View of
Proof of Concept
Test Area

Mutch Associates, LLC
Environmental Engineers and Scientists

Figure 3-2

Cross Section A-A'

Mutch Associates, LLC
Environmental Engineers and Scientists

VENTED CAP WITH LOCK

VENTED CAP

PROTECTIVE CASING

CONCRETE COLLAR

6"

GROUT MIXTURE OF BENTONITE AND PORTLAND CEMENT

BENTONITE SEAL (2 FEET MINIMUM)

SAND PACK

BOREHOLE

2 INCH DIAMETER PVC WELL SCREEN

THREADED BOTTOM CAP

VARIABL LENGTH

SAND PACK 2 FT ABOVE SCREEN

5 FT WELL SCREEN

NOT TO SCALE
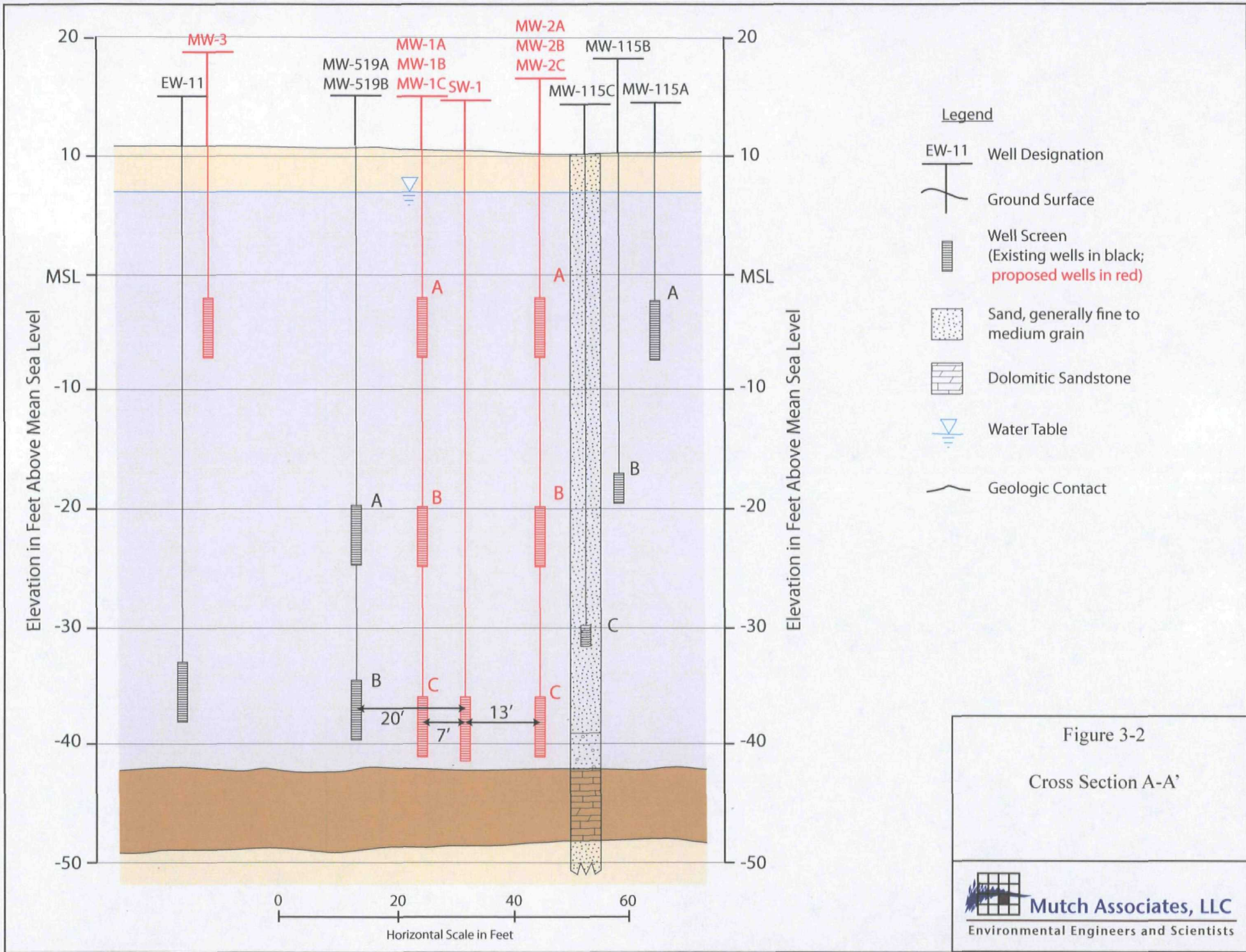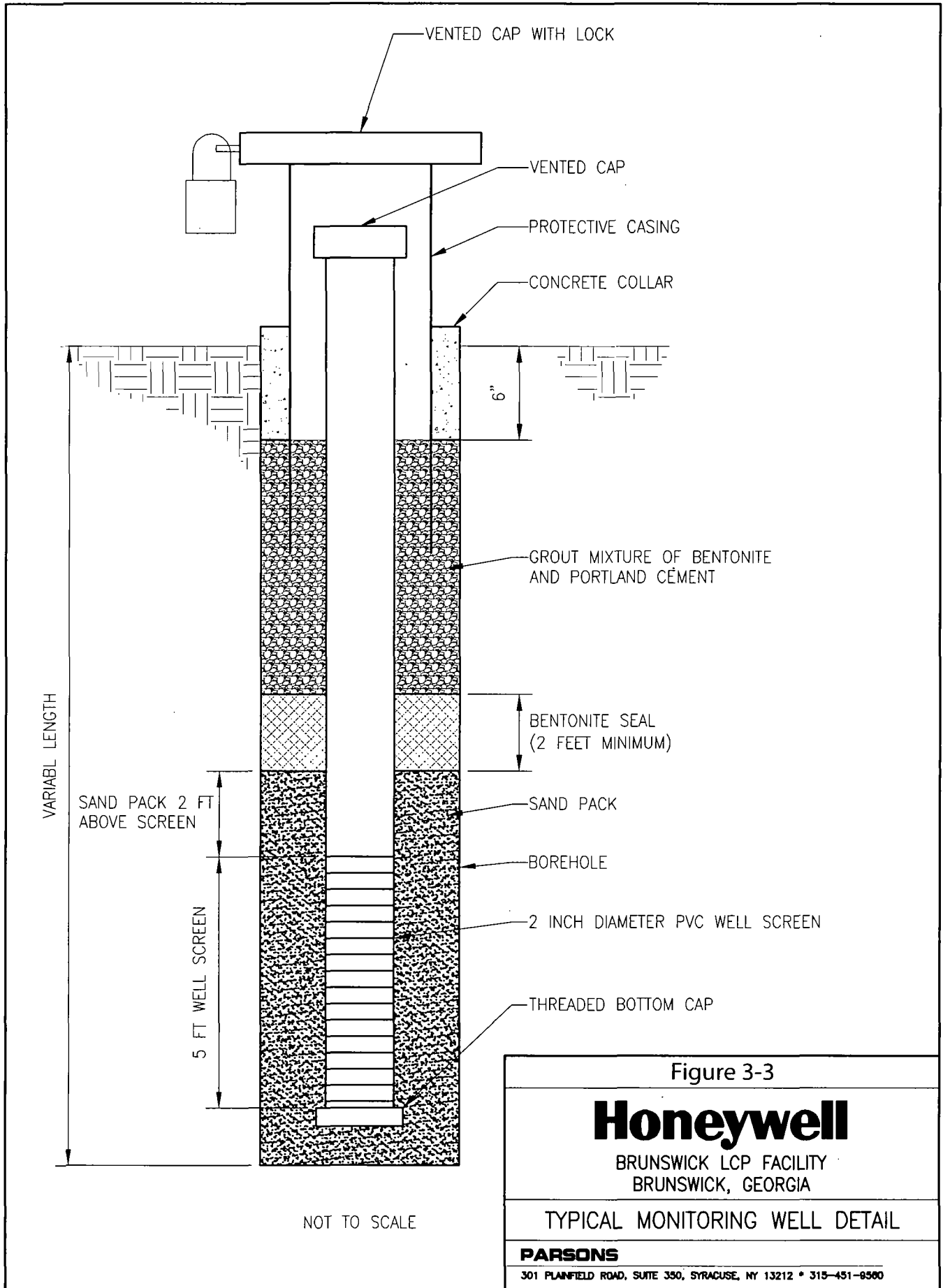
Figure 3-3

Honeywell

BRUNSWICK LCP FACILITY
BRUNSWICK, GEORGIA

TYPICAL MONITORING WELL DETAIL

PARSONS
301 PLAINFIELD ROAD, SUITE 350, SYRACUSE, NY 13212 • 315-451-9560

LEGEND:
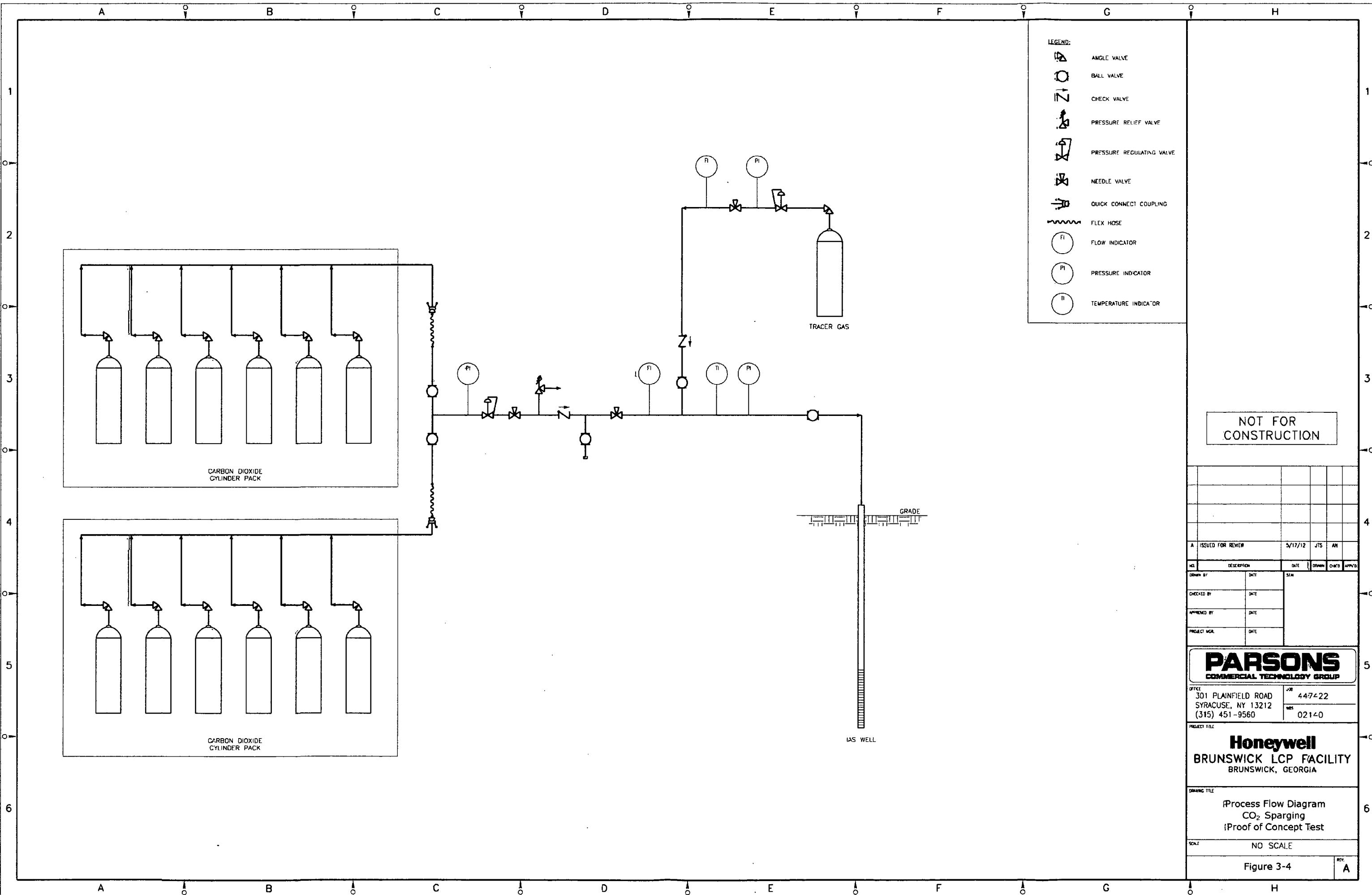
Symbol	Description
∠	ANGLE VALVE
⌀	BALL VALVE
⋈	CHECK VALVE
⋈	PRESSURE RELIEF VALVE
⋈	PRESSURE REGULATING VALVE
⋈	NEEDLE VALVE
⊣	QUICK CONNECT COUPLING
∿∿∿	FLEX HOSE
FI	FLOW INDICATOR
PI	PRESSURE INDICATOR
TI	TEMPERATURE INDICATOR

TRACER GAS

CARBON DIOXIDE
CYLINDER PACK

CARBON DIOXIDE
CYLINDER PACK

GRADE

GAS WELL

NOT FOR
CONSTRUCTION

NO	DESCRIPTION	DATE	DRAWN	CHK'D	APP'VD
A	ISSUED FOR REVIEW	5/17/12	JTS	AN	

DRAWN BY / DATE
CHECKED BY / DATE
APPROVED BY / DATE
PROJECT MGR. / DATE

PARSONS
COMMERCIAL TECHNOLOGY GROUP

OFFICE	JOB
301 PLAINFIELD ROAD	447422
SYRACUSE, NY 13212	WBS
(315) 451-9560	02140

PROJECT TITLE

Honeywell
BRUNSWICK LCP FACILITY
BRUNSWICK, GEORGIA

DRAWING TITLE
Process Flow Diagram
CO₂ Sparging
Proof of Concept Test

SCALE   NO SCALE

Figure 3-4   REV. A
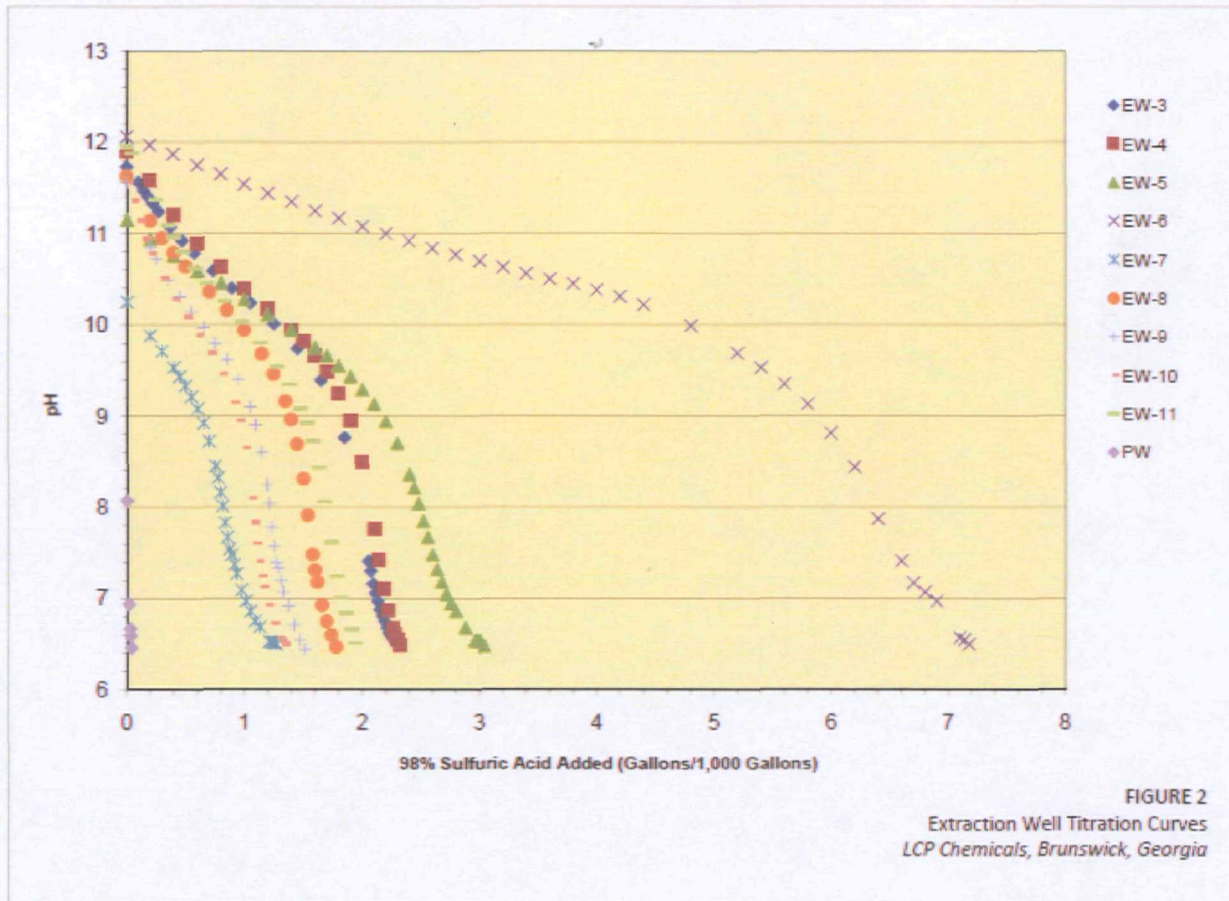
FIGURE 2
Extraction Well Titration Curves
LCP Chemicals, Brunswick, Georgia

Figure 3-5

CBP Titration Curves from
Remedial Investigation Report

Mutch Associates, LLC
Environmental Engineers and Scientists

(from CH2M Hill, 1997)
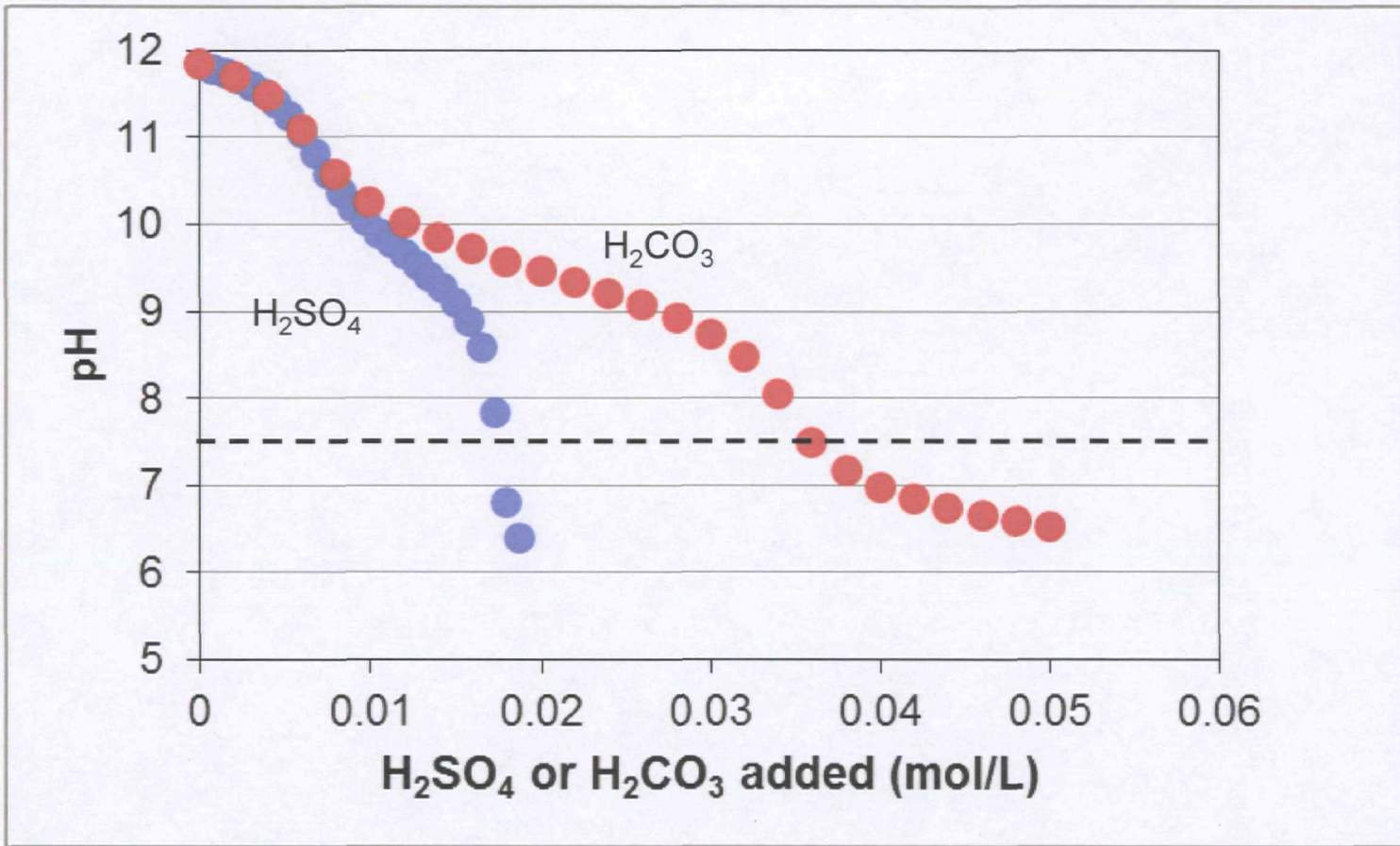
Figure 3-6

Numerical titration Curves for Water Collected from EW-4

Mutch Associates, LLC
Environmental Engineers and Scientists

Schedule for Brunswick CO_2 Proof of Concept Test

Task	Duration	Week 1 9/17	2 9/24	3 10/1	4 10/8	5 10/15	6 10/22	7 10/29	8 11/5	9 11/12	10 11/19	11 11/26	12 12/3	13 12/10	14 12/17	15 12/24	16 12/31	17 1/7	18 1/14	19 1/21	20 1/28	21 2/4	Week 22 2/11
Construction of sparge well and additional monitoring wells	3 wk	▓	▓	▓																			
Site surveying	1 wk			▓																			
Monitoring of water levels via transducers	8 wk			▓	▓	▓	▓	▓	▓	▓	▓												
Pre-sparge well sampling for water quality analysis	5 d				▓																		
Pre-sparging aquifer testing	1 wk					▓																	
Temporary injection equipment design and set-up	2 wk					▓	▓																
CO_2 sparging	3 wk								▓	▓	▓												
Continuous monitoring of pH and water levels	4 wk								▓	▓	▓	▓											
Post-sparge well sampling for water quality analysis	1 wk											▓											▓
Post-sparging aquifer testing	2 wk												▓	▓									
Reporting	18 wk			▓	▓	▓	▓	▓	▓	▓	▓	▓	▓	▓	▓	▓	▓	▓	▓	▓	★		

Legend

★ Draft Report

* Post-sparge well sampling is scheduled to occur 3 months and 6 months after conclusion of the test. The 6 month sampling round is not shown on the schedule. It will be performed on the week of 5/13/13.